DOE/JPL/954334-5

LOW COST SILICON SOLAR ARRAY PROJECT

Quarterly Progress Report, October—December 1977

By
W. C. Breneman
H. Cheung
E. G. Farrier
H. Morihara

Work Performed Under Contract No. NAS-7-100-954334

Union Carbide Corporation
Tarrytown, New York

U.S. Department of Energy

Solar Energy

DISCLAIMER

NOTICE

This report has been reproduced directly from the best available copy.

Available from the National Technical Information Service, U. S. Department of Commerce, Springfield, Virginia 22161.

Price: Paper Copy $6.00
Microfiche $3.00

DOE/JPL/954334-5
Distribution Category UC-63b

LOW COST SILICON SOLAR ARRAY PROJECT SILICON MATERIALS TASK

ESTABLISHMENT OF THE FEASIBILITY OF A PROCESS CAPABLE OF LOW-COST, HIGH-VOLUME PRODUCTION OF SILANE (Step I) AND THE PYROLYSIS OF SILANE TO SEMICONDUCTOR-GRADE SILICON (Step II)

JPL Contract 954334

QUARTERLY PROGRESS REPORT

Period Covered: October-December, 1977

W. C. Breneman
H. Cheung
E. G. Farrier
H. Morihara

UNION CARBIDE CORPORATION

TABLE OF CONTENTS

TABLE OF CONTENTS (Cont'd)

LIST OF ILLUSTRATIONS

TABLES

FIGURES

ABSTRACT

SILANE PRODUCTION

Kinetics and equilibria for the hydrogenation of silicon tetrachloride have shown that conversion to trichlorosilane is substantially increased at higher operating pressures; these results greatly improve the practicality of the overall process. Yields of 25% at 790 Kpa (100 psig) were achieved at reaction times of under 15 seconds. The use of low-cost cement copper as a hydrogenation catalyst has shown substantially identical kinetics as earlier copper/silicon alloys.

An integrated process development unit for converting metallurgical silicon and hydrogen to high-purity silane has been commissioned. Initial operation of the individual elements has followed designed performance. The hydrogenation section has been operated at up to 200 Kpa (275 psig) and has yielded equilibrium conversions to trichlorosilane at under 15 second residence time. Initial corrosion studies have ruled out titanium as a construction material for the hydrogenation reactor at 500°C. Inconel 625 or 316 stainless steel are likely candidates pending further tests.

SILICON PRODUCTION

A quartz fluid-bed reactor capable of operating at temperatures of up to 1000°C was designed, constructed, and successfully operated. During a 30-minute experiment, silane was decomposed within the reactor with no pyrolysis occurring on the reactor wall or on the gas injection system. A hammer-mill/roller-crusher system appeared to be the most practical method for producing seed material from bulk silicon.

A total of 6.7Kg of silicon powder was produced in two separate experiments in the free-space reactor without opening the reactor between experiments. No semi-solid growth formations were observed on either the gas injector or on the reactor wall. In one experiment, a silicon powder production rate of 2.8Kg/hr was maintained for one hour. The average particle size of the silicon powder was increased from the typical submicron size to approximately 1.3μm through modifications in the free-space reactor; non-spherical particles as large as 50μm were identified.

No measurable impurities were detected in the silicon powder produced by the free-space reactor, using the cathode layer emission spectroscopic technique. Impurity concentration followed by emission spectroscopic examination of the residue indicated a total impurity level of 2 micrograms/gram. A pellet cast from this powder had an electrical resistivity of 35-45 ohm-cm and P-type conductivity.

A 152mm-diameter melt consolidation apparatus was attached to the free-space reactor. During a run in which powder was pneumatically transferred from the free-space reactor to the hopper of the melt consolidator, a transfer and melting rate of 0.8Kg/hr was obtained. Rods suction-cast from this melt had P-type conductivity and average electrical resistivity of 35 ohm-cm.

PROCESS DESIGN

The first objective for the overall process was the definition of a preliminary set of functional specifications. All process design efforts are based on these specifications. For the silane production process, a Distillation Silane Process was formulated. The main feature of this process is the addition of a distillation column and a redistribution reactor to the tail-end of the process train to handle exclusively monochlorosilane. This feature will produce ultra-pure silane without an activated-carbon trap, according to calculations. The process design work will be carried out on both the original process (Adsorption Silane Process - ASP) and on the Distillation Silane Process (DSP); the relative merits of ASP and DSP were evaluated and the study, so far, slightly favors the latter process. The final process scheme selection will be made in early January.

Preliminary block flow diagrams and heat and material balances for every battery-limit stream were completed for the 25 MT/year experimental facility. Work on preliminary process flow diagrams and heat and mass balances for all process streams are in progress.

A brief parametric study was conducted to select an optimum range of operating pressures for the distillation columns. As a result, a pressure range of 35-50 psig is recommended for the TCS/STC column and 300-400 psig for all other columns. For DSP the process design for the first three columns has been completed using the recommended pressures.

Conceptual designs have been initiated for the hydrogenation reactor, the free-space reactor, and the consolidation system. The process design data available in-house and in the open literature reveal that additional data need to be acquired to perform a reliable heat and mass balance of the process. A preliminary list of needed data was compiled. A final list and a recommended data-acquisition program will follow.

In the fluidized-bed heating area, the first series of short experiments in a steel-wall reactor produced a bed temperature of above 100°C, indicating that fluidized particles can be heated by high-frequency capacitive heating. As the bed temperature was increased a sudden, unexplained, drop in bed impedance at 32°C was observed. Testing with a glass-wall reactor was started and we were able to heat the bed in the fluidized state; testing will center on determining fluidization regimes and electrical characteristics. Tests were also run with the center electrode coated with ceramic cement; the coating maintained its electrical integrity throughout the test. The electrodes will eventually be coated with silicon or silica in order to minimize contamination. The theoretical model has been incorporated into a computer program to determine regimes of stability and optimum operating conditions.

1.0 SILANE PRODUCTION

1.1 INTRODUCTION

The purpose of this program is to determine the feasibility and practicality of high-volume, low-cost production of silane (SiH_4) as an intermediate for obtaining solar-grade silicon metal. The process is based on the synthesis of SiH_4 by the catalytic disproportionation of chlorosilanes resulting from the reaction of hydrogen, metallurgical silicon, and silicon tetrachloride. The goal is to demonstrate the feasibility of a silane production cost of under $4.00/kg at a production rate of 1000 MT/year.

Prior to the inception of this program in October 1975, Union Carbide had shown that pure hydrochlorosilanes could be disproportionated to an equilibrium mixture of other hydrochlorosilanes by contact with a tertiary-amine, ion-exchange resin. In addition, Union Carbide had shown that silicon tetrachloride, a by-product of silane disproportionation, can be converted to trichlorosilane with metallurgical silicon metal and hydrogen.

Thus, a closed-cycle purification scheme was proposed to convert metallurgical-grade silicon into high-purity, solar-grade silicon using hydrochlorosilanes as intermediates. This process appears as:

1. Hydrogenation of metallurgical silicon metal and of by-product silicon tetrachloride to form trichlorosilane.

   $$2\ H_2 + 3\ SiCl_4 + Si\ (M\text{-}G) \xrightarrow[Cu]{550} 4\ HSiCl_3$$

2. Disproportionation of trichlorosilane to silane and silicon tetrachloride.

   $$4\ HSiCl_3 \longrightarrow 3\ SiCl_4 + SiH_4$$

3. Pyrolysis of silane to high-purity silicon.

   $$SiH_4 \xrightarrow{Heat} Si + 2H_2$$

Until now, laboratory investigations have defined the rate, equilibrium conversion, and certain mechanistic aspects of the disproportionation and hydrogenation reactions at atmospheric pressure. A small process-development unit, capable of operating under pressure, was constructed and operated to demonstrate the conversion of dichlorosilane to silane. The unit has confirmed laboratory findings and has routinely produced high-quality silane in good yield.

The construction of a high-pressure hydrogenation unit and of an integrated silane and hydrogenation unit was also completed during this last quarter.

1.2 DISCUSSION

1.2.1 HYDROGENATION STUDIES

The hydrogenation of silicon tetrachloride, which produces trichlorosilane while consuming metallurgical silicon metal, is a key feature of the low-cost silane process. It is by this reaction that the metallurgical silicon is converted into easily purified, low-boiling chlorosilanes. During the past quarter, two major efforts were in progress more precisely to define a workable process. A laboratory program was undertaken to study the process chemistry with respect to equilibrium, kinetics, and copper catalyst. The second effort was the demonstration of the process on a larger scale to delineate potential scale-up problems and to expand the data base.

Several workers have studied the H-Si-Cl system at elevated temperatures (circa 1100 K), as part of the manufacture of high-purity silicon, in order to elucidate the observed etching or deposition of silicon metal. While the kinetics at high temperatures permit a relatively rapid approach to equilibrium, at lower temperatures the uncatalyzed reaction is slow and heretofore of little interest— especially since the major thrust was to develop silicon deposition techniques. Early work at Union Carbide had established that proper catalysts could enhance the kinetics and that silicon tetrachloride (STC) could, in fact, be converted to trichlorosilane (TCS). The present work extends that concept.

In the chemical system under study, it is assumed that only two phases are present — gaseous and solid. With three components — silicon, hydrogen, and chlorine — the phase rule demands three degrees of freedom. After choosing temperature and pressure, the next practical choice is the hydrogen/chlorine ratio in the gas phase as it is the only quantity which remains constant regardless of the extent of reaction, (i.e., neither the H nor Cl flux is altered by the deposition or etching of silicon). Thus, a unique equilibrium composition should exist if temperature, pressure, and H/Cl ratio are specified. For the system of practical interest in which dichlorosilane (DCS), TCS, STC, and H_2 are the only significant products, (Cl_2, $SiCl_2$, HCl and other compounds could also be present but at levels too low to impact the overall system) the following expressions can be written:

$$Si + 3HCl \longrightarrow HSiCl_3 + H_2 \qquad (1)$$

$$Si + 4HCl \longrightarrow SiCl_4 + 2H_2 \qquad (2)$$

$$Si + 2HCl \longrightarrow H_2SiCl_2 \qquad (3)$$

Or, in terms of the components which are present in amounts large enough to measure experimentally,

$$Si + 2H_2 + 3SiCl_4 \longrightarrow 4HSiCl_3$$

$$Si + 2H_2 + SiCl_4 \longrightarrow 2H_2SiCl_2$$

Thus, the appropriate equilibrium expressions would be:

$$K_{p_1} = (P_{HSiCl_3})^4/(P_{SiCl_4})^3 \ (P_{H_2})^2$$

$$K_{p_2} = (P_{H_2SiCl_2})^2/(P_{SiCl_4}) \ (P_{H_2})^2$$

1.2.1a LABORATORY STUDIES

Since the hydrogenation reactions yield fewer moles of gaseous compounds as the reaction proceeds, increasing the pressure should increase conversion. Earlier studies under the present contract were conducted at atmospheric pressure. Recently, a laboratory fluidized-bed reactor was constructed to permit studies at pressures up to 770 Kpa (112 psia). In the current period, this reactor was used to determine the equilibrium composition at various hydrogen-to-chlorine ratios, temperatures, and pressures.

A summary of the data obtained from the laboratory reactor is shown in Table 1.1. After calculating the equilibrium constant K_p for TCS and DCS at each temperature, pressure, and H/Cl ratio, the values at constant temperature were compared. These indicated consistent values are independent of H/Cl ratio and pressure, as would be expected. The beneficial effect of pressure was also observed as conversions of up to 25% were seen at 770 Kpa (112 psia). An estimate of the heat of

Table 1.1

SUMMARY OF EQUILIBRIUM CONSTANTS FOR THE HYDROGENATION OF $SiCl_4$

Temp. (°C)	Pressure (Kpa)	H/Cl Ratio	H_2SiCl_2 (Mole %)	$HSiCl_3$ (Mole %)	$SiCl_4$ (Mole %)	K_{p_1} (atm^{-1})	K_{p_2} (atm^{-1})
450	770	.43	.273	16.90	82.83	$.64 \times 10^{-3}$	4.04×10^{-6}
450	770	.85	.407	22.11	77.50	.76	3.15
450	770	1.25	.510	23.31	76.18	.57	2.91
450	448	.65	.201	17.45	82.35	.61	1.79
450	448	1.30	.326	20.75	78.92	.52	1.84
						.62 ± .09	2.74 ± .95
500	770	.42	.369	19.48	80.19	1.30	7.96
500	770	.85	.557	23.49	75.45	1.16	6.18
500	770	1.25	.681	26.71	72.61	1.16	5.59
500	448	.65	.300	20.14	79.57	1.23	4.26
500	448	1.30	.366	22.46	78.07	.73	2.35
						1.12 ± .22	5.27 ± 2.10
550	770	.42	.391	19.82	79.78	1.44	9.04
550	770	.85	.635	25.10	74.26	1.47	8.26
550	770	1.25	.668	26.98	72.35	1.22	5.41
550	448	.65	.300	10.01	79.62	1.21	4.26
550	448	1.30	.368	24.08	75.55	1.09	2.50
						1.29 ± 16	5.89 ± 2.73

$$K_{p_1} = \frac{(P_{HSiCl_3})^4}{(P_{H_2})^2 \quad (P_{SiCl_4})^3}$$

$$K_{p_2} = \frac{(P_{H_2SiCl_2})^2}{(P_{H_2})^2 \quad (P_{SiCl_4})}$$

reaction to form TCS and DCS was made by plotting the variation of equilibrium constant with temperature (Figure 1.1). Using a least-squares fit of a function, lnKp vs. 1/T, the heat of reaction was determined as the slope of the line. The values of +8.3 and +9.1 kcal/mole Si are consistent with the observed increased conversion at higher temperatures. The values do not agree with the JANAF tables but do agree with more recent data (Hunt and Sirtl, J. Elect. Soc. 119 p. 1741, 1972) which give -116 kcal/mole as the heat of formation of TCS, compared to the JANAF value of -112 kcal/mole.

The kinetics of the hydrogenation reaction were briefly investigated during this period as an adjunct to the equilibrium determinations. Several experiments at 500°C, 65 psia, and short gas residence times were conducted and compared with similar experiments performed at the beginning of the equilibrium study; the same copper/silicon mass was used throughout. This recheck, shown in Figure 1.2, indicated no significant change in reaction rate between the initial and final experiment. Substantial equilibrium was achieved in less than twenty seconds, the initial reaction being esentially first order.

A mass balance was carried out by comparing the weight of silicon remaining in the reactor with the original charge and with the quantity of reactants introduced. The prod-

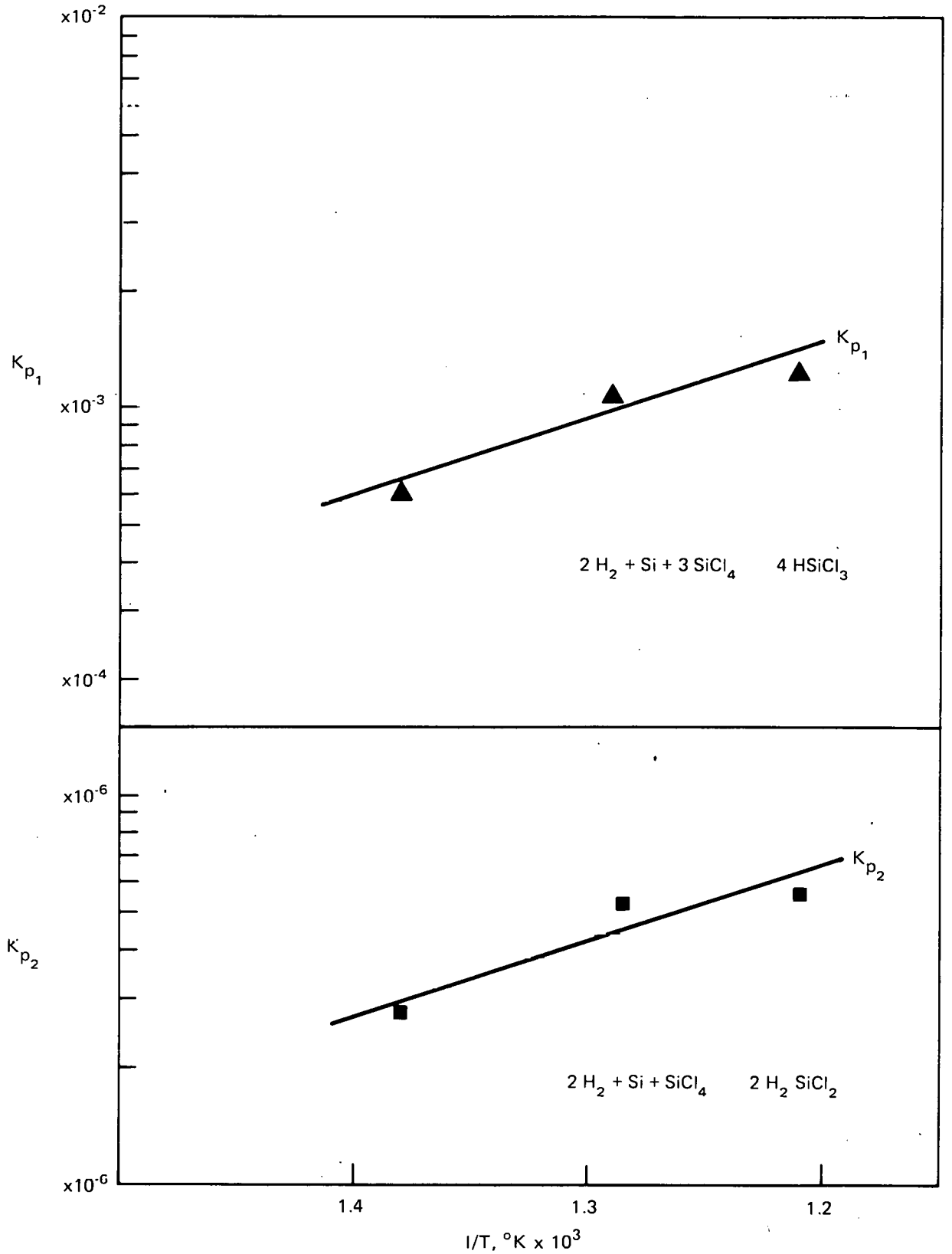

Figure 1.1
EQUILIBRIUM CONSTANT vs TEMPERATURE

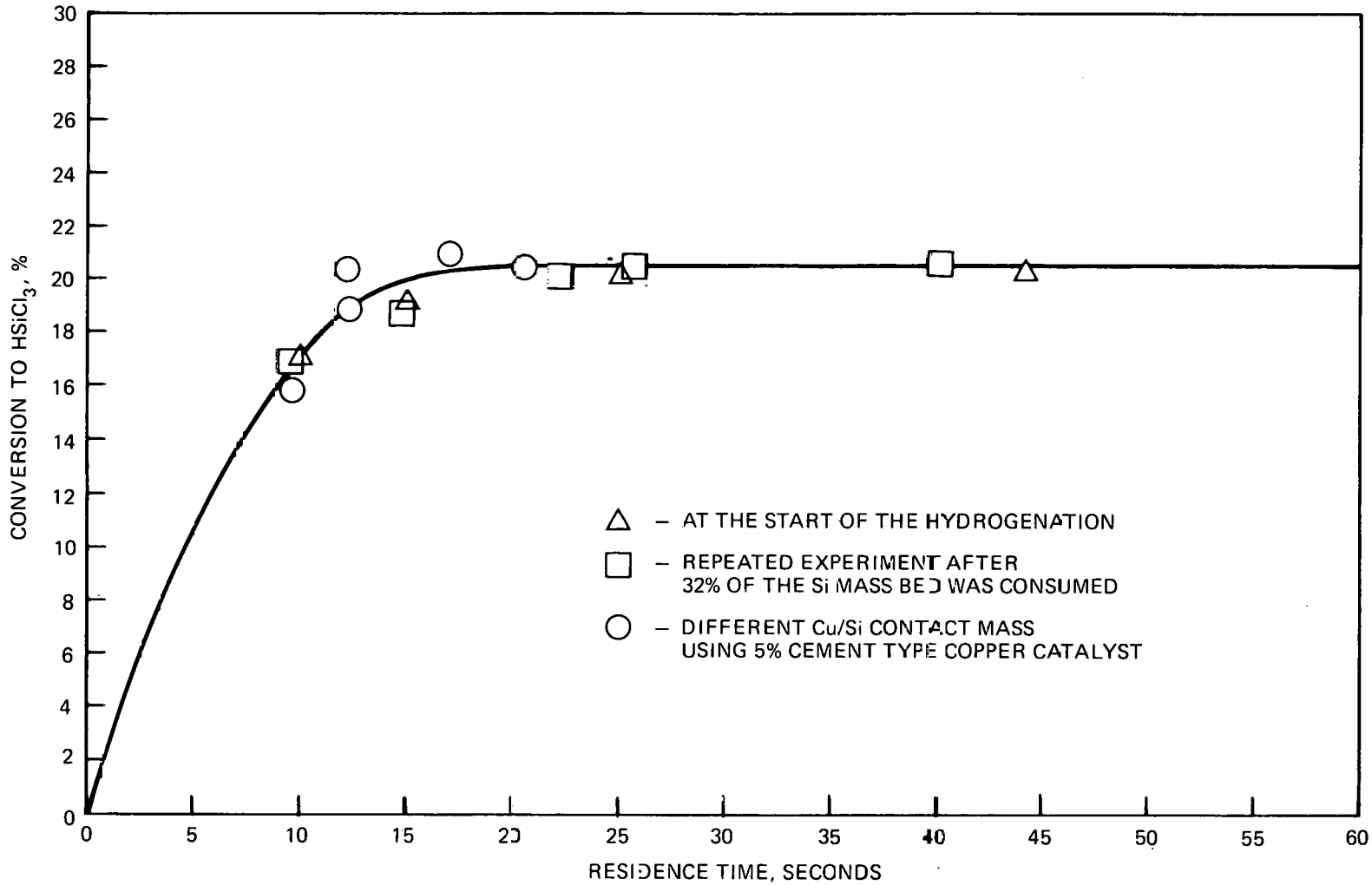

Figure 1.2
HYDROGENATION OF $SiCl_4$ TO $HSiCl_3$ AT 448 kPa
AND 0.65 H/Cl RATIO AT 500°C

ucts collected gave an overall closure of 92%. The 5-gram deficit of silicon equivalent is most likely accounted for by the elutriation of fines lost in the condensate and filter system which were coated with a thin film of material. The residual copper/silicon mass showed an increase in copper content from 2.9% to 3.9% over the experimental period. Thus, while 33.7% of the initial silicon was consumed, only 21.1% of the copper was lost. More complete analysis of the used silicon is in progress and will aid in understanding the mechanism of the copper-silicon interaction during the life of the mass and will allow prediction of copper-utilization efficiency. The vent gas (unreacted hydrogen) was collected and analyzed by mass spectrograph. It consisted of essentially pure hydrogen with less than 20 ppm hydrogen chloride.

The copper/silicon contact mass used in the fluid-bed hydrogenation reactor has, until now, been in the form of a copper/silicon alloy containing about 3% metallic copper. The preparation of this material would have required a separate process step or the purchase of a special raw material. To achieve a simple, one-step catalyst system and to help understand the role of the catalyst, a cement-type copper was evaluated in a mixture with metallurgical silicon and used without further treatment at 500°C with hydrogen/STC vapor. The cement copper material is a commercially available, low-cost mixture of copper

metal and copper oxides with a particle size averaging 8.3 microns and having a surface area of about 4 m^2/g. A detailed analysis is listed in Table 1.2 and indicates a copper content of 78.5 wt %.

A blend of 5% cement copper with metallurgical silicon — for a total of 3.9 wt % copper — was reacted with a 1.3:1 molar ratio of hydrogen and STC at 500°C and 65 psia. The gas flow was started slowly to avoid possible elutriation of small copper particles and then increased as the composition of the condensate indicated substantial reaction. Steady-state operation was achieved after eight hours, with equilibria and gross kinetics identical to those previously obtained with a 3-4% copper/silicon alloy mass (Figure 1.2). During the initial period, a significant amount of high-boiling compounds were formed which diminished to the normal level of $< 0.05\%$ at steady state. These heavies could be attributed to the generation of water in the reduction of the copper oxides and to the subsequent hydrolysis of chlorosilanes:

$$CuO + H_2 \longrightarrow Cu + H_2O$$

$$H_2O + SiCl_4 \longrightarrow SiO_2 + HCl$$

The HCl so formed would react with the metallurgical silicon forming either $SiCl_4$ or $HSiCl_3$. The favorable results of these experiments indicate that low-cost, readily available cement

copper can be effectively used as the hydrogenation catalyst. Work in progress will seek to define the catalyst level required for most economic operation.

1.2.1b PROCESS DEVELOPMENT UNIT

A hydrogenation reactor utilizing a 7.6 cm-diameter and 120 cm-high fluid-bed reactor was constructed to study reaction variables on a larger scale and to provide feed material for the subsequent redistribution/distillation system. Initial activities during this period involved debugging the system and performing preliminary experiments necessary for the subsequent experimental program. By the end of the quarter, the mechanical operation had been proven to the point where reliable equilibrium, kinetic, and other operational data could be obtained at pressures of up to 2000 Kpa (275 psig) and temperatures of up to 550^{o}C. Several preliminary runs were carried out to prepare a sufficient quantity of copper/silicon contact mass for the planned experimental program. This material was then used to hydrogenate STC. The results from this initial set of experiments showed, as expected, the formation of a considerable quantity of TCS at short reaction times (Table 1.3).

1.2.2 INTEGRATED PROCESS SYSTEM

The production of silane from trichlorosilane generates co-product silicon tetrachloride. The hydrogenation of STC to TCS recycles this co-product and holds the potential

Table 1.2
TYPICAL COMPOSITION
OF CEMENT COPPER

Copper	8.8 %
Cuprous Oxide	68.2
Cupric Oxide	11.4
Iron	3.2
Aluminum	0.18
Magnesium	0.4
Lead	0.08
Arsenic	0.10
Sulfates	2.00
Total Copper	78.5
Surface Area	3.9 m^2/g
Mean Diameter	8.3 microns

Table 1.3
PRELIMINARY RESULTS FROM HYDROGENATION UNIT
AT 790 Kpa, RATIO H/Cl 4.25

Reaction Temperature °C	Residence Time Seconds	Product Composition, Mole % $HSiCl_3$	$SiCl_4$
474	3.9	14.1	85.9
482	3.9	9.6	90.4
659	3.9	14.4	85.6
390	5.2	10.8	89.2
401	5.2	12.4	87.6
409	5.2	12.2	87.8
420	5.2	13.2	86.8
445	5.2	10.9	89.1
475	7.8	8.8	91.2
517	7.8	7.1	92.9
485	11.7	15.3	84.7
510	11.7	18.5	81.5
559	11.7	20.1	79.9

for an integrated metallurgical silicon-to-silane process requiring only hydrogen as an additional raw material. Previously, a dichlorosilane-to-silane unit demonstrated the practicality of this final step in silane synthesis; during this period, the construction of a unit to couple the hydrogenation reactor with the silane-producing section was completed and start-up activities were initiated. The unit, described in detail in the previous report, consists of a distillation column for fractionating TCS from STC and of a disproportionation reactor to convert essentially pure TCS to an equilibrium mixture of di-, tri-, and tetrachlorosilanes. When fully integrated, this unit will yield dichlorosilane (DCS) from the crude TCS/STC produced in the hydrogenation section and will recycle STC to the hydrogenation reactor.

The ion-exchange resin catalyst (Amberlyst A-21) used in the disproportionation reactor is received as a water-saturated material in free-base form. Prior to contact with chlorosilanes, it is extracted with ethanol to remove the water and flushed with trichlorofluoromethane to remove the alcohol. After evaporation of the fluorocarbon, silicon tetrachloride is used to saturate the resin and to dry any residual moisture in the unit.

The major activity during this period was to assure the proper mechanical and control action of the system

under actual load, prior to its integration into the total system. This was accomplished. The initial trichlorosilane feed through the disproportionation reactor was converted to near-equilibrium amounts of DCS/TCS and STC (10-80-10 ratio); the distillation column, although not operating under optimum conditions, did adequately separate the various fractions. Some minor difficulties that were encountered and resolved dealt with the trichlorosilane feed pump and with temperature and pressure control on the reactor. In the latter case, operation near the boiling point of the TCS feed resulted in vapor formation inside the reactor due to TCS conversion to DCS. This caused increased pressure drop and unstable operation. Raising the operating pressure has resolved the problem and a preliminary material balance around the unit showed 97-99% closure despite the somewhat unstable initial operation and system hold-up.

1.2.3 CORROSION STUDIES

Although chlorosilanes are not corrosive to carbon steel, stainless steel, or to other common metals at normal temperatures, the amine-functional resin used as a disproportionation catalyst can exist as the amine-hydrochloride and could, therefore, be corrosive to steel. In addition, the high temperature environment of the hydrogenation reactor coupled with the potential presence of hydrogen chloride further underlines the necessity for choosing appropriate materials of construction.

Consequently, a rack of corrosion test specimens was installed in both the hydrogenation reactor and in the TCS disproportionation reactor prior to start-up. For the disproportionation reactor, carbon steel and "316" and "304" stainless steels were selected. This selection was based on the good performance to date with the 316 S.S. reactor handling DCS and with the commercial-scale TCS converter.

The hydrogenation reactor was equipped with specimens of carbon steel, 316 S.S., 304 S.S., Inconel 625, titanium and 3RE-60 nickel alloy. One set was installed in the vapor section above the fluidized bed and another set was immersed in the reaction zone. During preliminary start-up activities, a malfunction of a reactor-temperature controller caused the system to overheat to nearly 900°C. The corrosion rack was removed for examination after 15.5 hours of on-stream time (including the approximately two-hour temperature excursion). A preliminary examination of the test coupons showed that significant hard scale had formed on all specimens. The titanium coupons were virtually destroyed. The weight loss of specimens exposed only to the vapor was less than the weight loss of those in the copper/silicon fluidized reaction medium. All samples were corroded beyond tolerable limits for a practical reaction system.

The reactor tube itself, constructed of 304 S.S., did not appear to be attacked so as to weaken it or curtail our

experimental program. A new set of corrosion specimens is being prepared for testing and more pertinent corrosion data are expected because the temperature-control problem has been resolved.

1.3 CONCLUSIONS

- The rapid reaction rate and enhanced conversion of silicon tetrachloride as a result of increased reaction pressure demonstrates the feasibility of this critical step in the low-cost silane production scheme.

- The direct use of low-cost, readily available cement copper as a catalyst for the hydrogenation of silicon tetrachloride eliminates a separate catalyst preparation step.

- Titanium has been eliminated as a material of construction for the hydrogenation reactor. High-chromium steel alloys remain potential candidates.

- The hydrogenation of silicon tetrachloride is mildly endothermic (8.3 kcal/mole silicon).

1.4 PROJECTED QUARTERLY ACTIVITIES

1.4.1 LABORATORY ACTIVITIES

- Examine the role of copper in catalyzing the hydrogenation of silicon tetrachloride.

- Further define the kinetics of the hydrogenation reaction at low catalyst levels.

1.4.2 INTEGRATED PROCESS UNIT

- Examine kinetics of hydrogenation of silicon tetrachloride in a modest-scale pressure reactor.

- Integrate the hydrogenation and disproportionation units into a single processing chain.

- Demonstrate process integration over an extended operation period.

- Continue corrosion testing and materials evaluation.

2.0 SILICON PRODUCTION

2.1 INTRODUCTION

The objective of this program started in January 1977, is to establish the economic feasibility of manufacturing semiconductor-grade polycrystalline silicon by the pyrolysis of silane. The pyrolysis methods to be investigated involve fluid-bed and free-space processes.

In the development effort prior to the current quarter, engineering and design problems associated with the construction of a fluid-bed reactor for elevated-temperature use were identified. As a partial demonstration of the capabilities of a moderate-size reactor, the current free-space reactor was operated for five hours and shut down on schedule. Preliminary purity analyses were completed for powder samples from the free-space reactor and identified sources of impurities were eliminated. Equipment was designed and procurement and construction were started on a melt consolidator. The melt consolidator will be attached to the free-space reactor, and its powder will be pneumatically transferred from the free-space reactor to the melter. A pellet-casting technique was also developed to provide a tool for rapid product and process evaluation.

2.2 DISCUSSION

2.2.1 SILANE PYROLYSIS

2.21a FLUID-BED REACTOR

I. — Reactor Design and Behavior

A quartz fluid-bed reactor (85mm I.D.) with a flat-plate gas feed was designed and constructed for use at elevated temperatures. A schematic of the gas train for the reactor is shown in Figure 2.1. The current design of the water-cooled gas feed system consists of a centrally-positioned 2mm orifice surrounded by a porous-metal gas distributor (average pore size — 35 μm).

Figure 2.2 is a photograph of the quartz fluid-bed reactor, the gas-flow control panel, and the temperature recorder. A resistance heater surrounds the lower portion of the quartz reactor which contains the silicon seed bed along with the gas distributor. A graphite seal between the gas distributor and the quartz reactor prevents the seed bed from falling into the cold region below the distributor where an O-ring seal makes the reactor pressure-tight.

With the current gas distributor plate, gases can be introduced into the fluid-bed reactor through the flat, porous metal plate, through the central 2mm-diameter

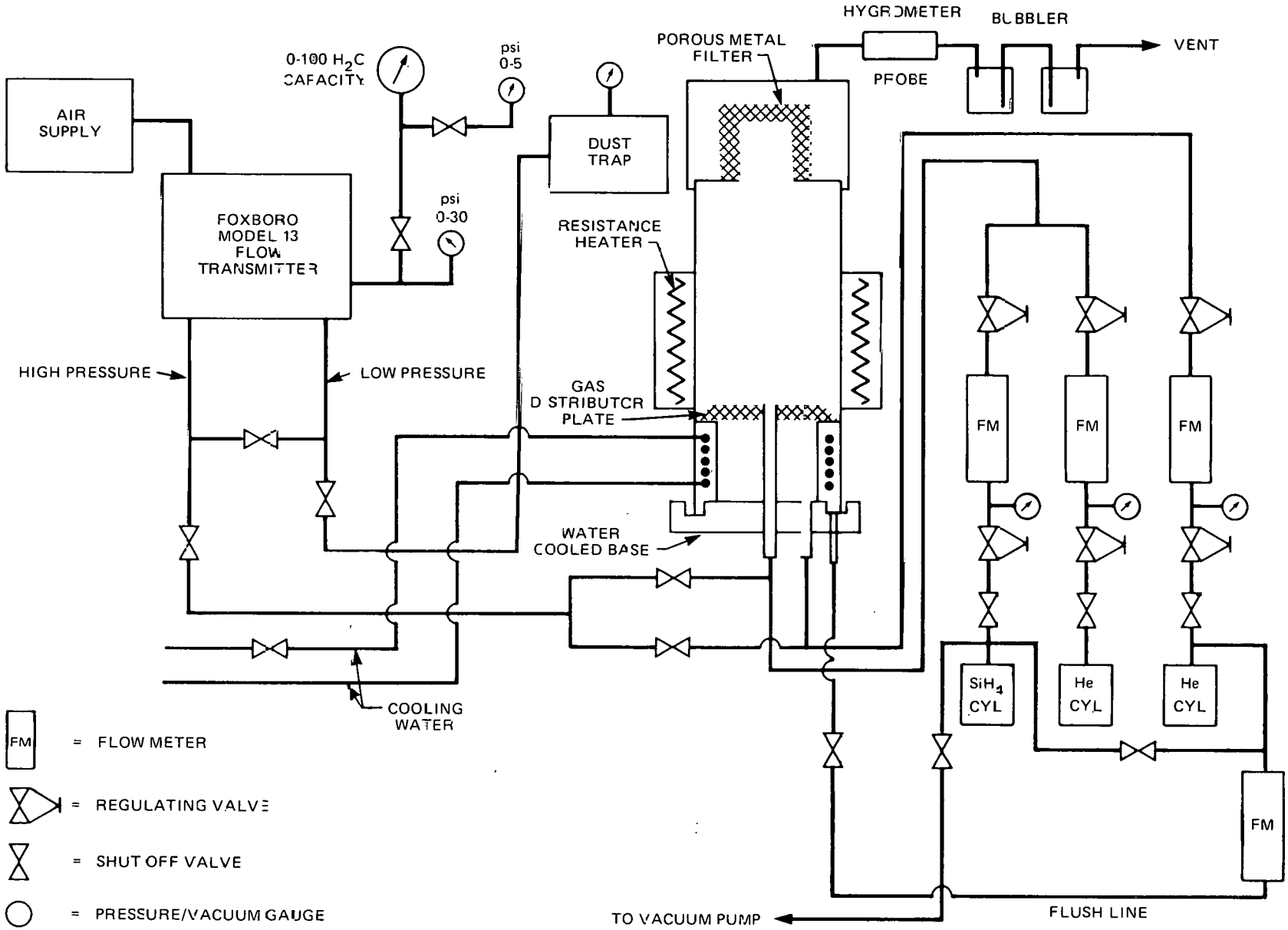

Figure 2.1

GAS-TRAIN SCHEMATIC FOR QUARTZ FLUID-BED REACTOR

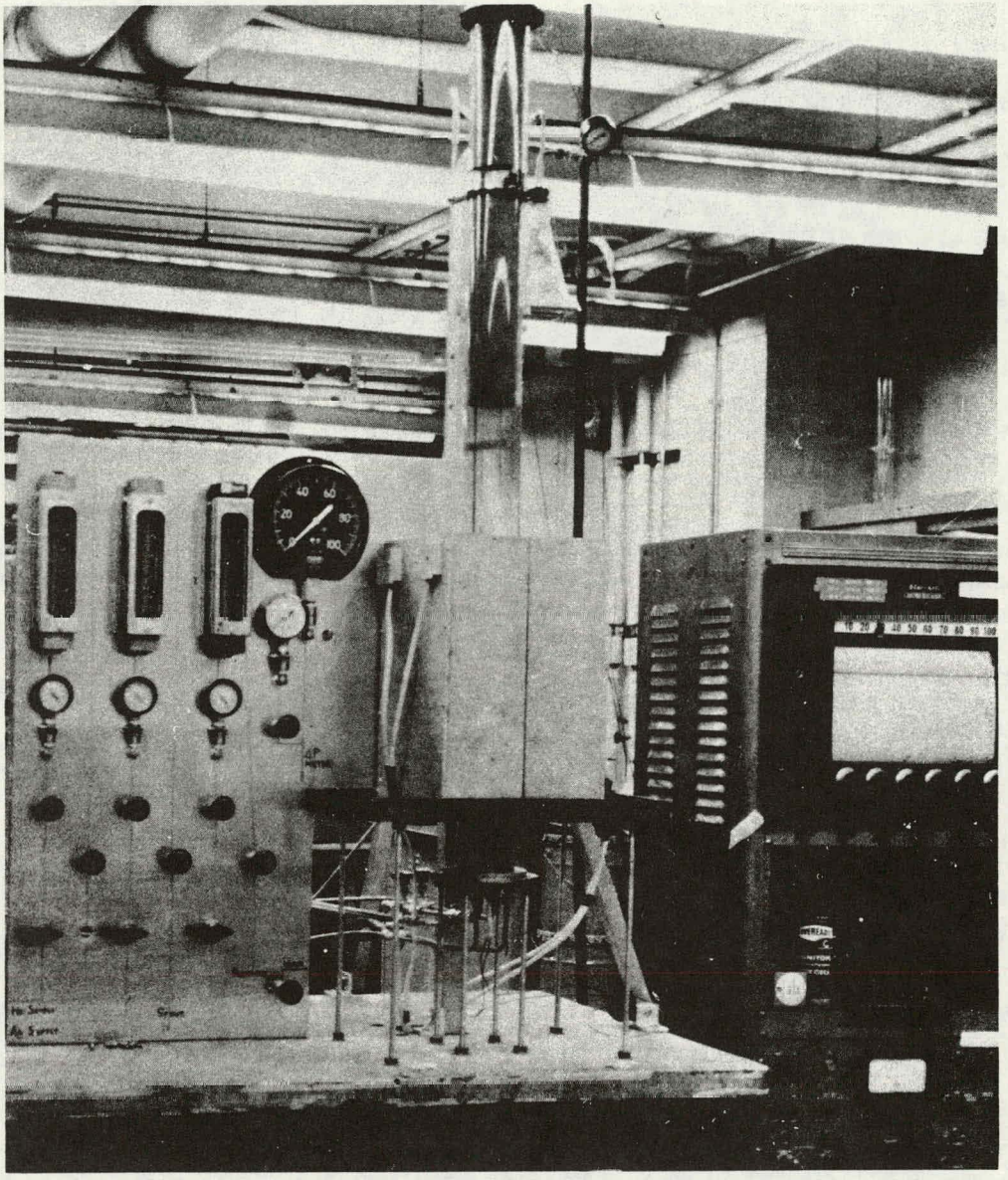

Figure 2.2
ASSEMBLY FOR QUARTZ FLUID-BED REACTOR

orifice, or simultaneously through both. A series of room-temperature experiments were conducted to observe the behavior of a bed of -35/+60 mesh silicon particles; helium was used as the fluidizing medium. For bed heights up to 200mm (the maximum examined), an active-bubbling bed (with occasional slugging) was obtained when helium was introduced solely through the porous metal plate; the maximum flow rates varied from 45 l/min for a 50mm-deep bed to 65 l/min for a 200mm-deep bed. When helium was injected through the central orifice alone, the helium flow rates needed to initiate a spouting action (stagnant bed below these rates) varied from 6 l/min to 30 l/min, respectively, for 50mm and 150mm-deep beds. For the 150mm-deep bed, the spout was unstable. No particle motion was observed in the annulus region of the spouting bed. A spout-fluidized bed was obtained for bed depths of up to 150mm under conditions where a constant 50 l/min of helium was fed through the porous metal plate while helium flow through the central orifice was varied. Spouting action was initiated in the fluidized bed at the same flow rates as those obtained without fluidization. The primary difference between spouting and spout-fluidized beds lies in the active motion of the particles in the annulus region of the bed. At room temperature, the current gas-distributor design was capable of providing stable beds with fluidized, spouting, and spout-fluidized actions.

In a preliminary series of elevated-temperature experiments conducted with helium, the bed behavior

was not so stable as at room temperature. With a 172mm-deep bed of particles, a spout-fluidized bed was established at a wall temperature of approximately 900°C. As the temperature continued to rise and approach 950°C, the particle motion became erratic. At 1000°C, the bed was slugging violently. With a 100mm-deep bed, a spout-fluidization was established at approximately 800°C; this stable condition was maintained to approximately 860°C. From 860 - 900°C, a dense layer of particles (approximately 1-5mm thick) started clinging to the reactor wall above the bed. The layer extended to a height of 400-500mm. Occasionally, part of the layer collapsed and fell into the spout-fluidized bed; the wall layer would then build up again. This recurring behavior prevented the establishment of a stable bed.

The first silane pyrolysis experiment was conducted in the unstable, 100mm-deep bed described above. The bed was fluidized with 50 l/min of helium fed through the porous metal plate; simultaneously, a mixture of helium and silane was injected through the central orifice. The helium flow rate through the orifice was held constant at 30 l/min while the silane flow rate varied from 1 to 5 l/min. The silane pyrolysis experiment was terminated after 30 minutes. With the reactor wall at 900°C, there was no evidence of silane combustion (white flame) at the exhaust port. A thorough examination of this system after cooldown revealed that no semi-solids formed

on the gas injector or on the reactor wall, nor were the particles agglomerated. Material losses prevented the determination of a mass balance; however, of the 70 grams of silicon theoretically produced, only 25 grams were recovered as fines. The remainder may have plated onto the original seed-bed particles. The products from the first fluid-bed pyrolysis experiment will be examined metallographically.

II. Seed Bed Source

A practical source of high-purity seed for the fluid-bed reactor may be obtained by crushing, classifying, and cleaning a portion of the fluid-bed reactor product. A hammer mill as well as jaw, cone, and roller crushers were evaluated as means of reducing bulk silicon to a specific particle size distribution. Metallurgical-grade silicon from Union Carbide (Lot #7893) was used. A known quantity of silicon was employed for every crushing method. After the first comminution, the particles were classified* by screening into specific size ranges. The particles remaining on the 35-mesh Tyler screen were returned to the same crusher and the process repeated. The data presented in Table 2.1 show the cumulative yield after three crushings and classifications. A 50% yield may be obtained, for particles in the 300 $\pm$100 m range, through the combined use of a hammer mill and a roller crusher.

---

* Screen analyses were carried out as described in ASTM-E-11-70.

The various particle sizes from each crushing operation were examined with a Scanning Electron Microscope (SEM). Figure 2.3 shows the typical acicular shape of all powders examined. Dry and wet tumbling in a 10.2cm-diameter rubber container were evaluated for converting the acicular material into more uniform particles. In the wet-tumbling operation, methanol and distilled water were added to the powder charge. SEM examination did not reveal any noticeable decrease in particle acicularity.

Table 2.1
CUMULATIVE YIELD FOR SEVERAL CRUSHING METHODS

Crushing Method	Feed Stock Size	Cumulative Yield for Mesh Size Listed			
		+35	35/60	60/100	-100
Roller Crusher*	1.3 cm to +35 mesh	1	37	31	31
Hammer Mill	10 cm to +35 mesh	23	43	20	14
Jaw Crusher	10 cm to +35 mesh	81	10	4	5
Cone Crusher	10 cm to +35 mesh	77	12	5	6

* The feed stock had to be reduced (via the jaw crusher) to the size indicated for acceptance through the roller crusher.

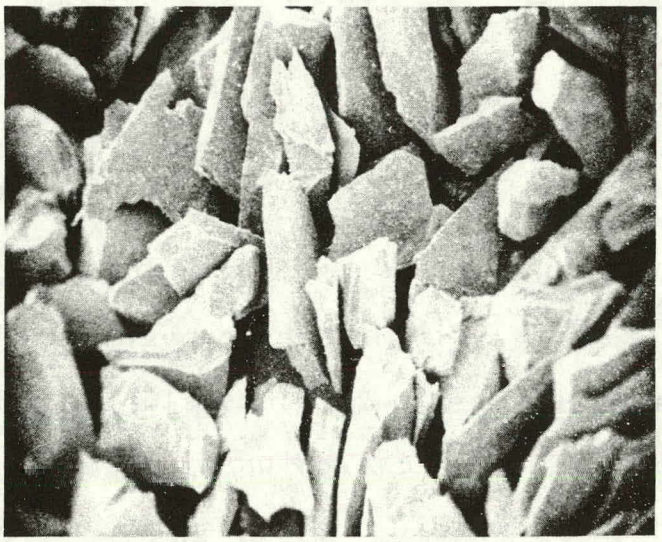

Figure 2.3
SEM PHOTOGRAPH OF CRUSHED 60/100 MESH
SILICON PARTICLES AT 50X MAGNIFICATION

2.2.1b FREE-SPACE REACTOR

I. – Purity

The current free-space process was critically examined in an effort to pinpoint possible sources of silicon contamination and to refine powder production and handling procedures. As a consequence, the entire system was cleaned and a purity experiment was conducted during which 2.4 kg of silicon powder was produced. Impurity analyses were obtained on powder samples taken at the beginning, middle, and toward the end of the experiment.

Two techniques were used to determine the level of impurities in these powders: the cathode layer

emission spectroscopic technique showed no detectable impurities, while the concentration technique* followed by emission spectroscopic examination detected the impurity levels shown in Table 2.2. The data established that the purity of silicon powder steadily improved as the run progressed.

Table 2.2
FREE-SPACE POWDER IMPURITY** ANALYSIS

	Estimated Powder Sampling Time***		
Element	90 min.	150 min.	200 min.
Al	1.4 ± 0.5	1.1 ± 0.5	0.6 ± 0.5
Ca	0.3 ± 0.3	0.3 ± 0.3	0.3 ± 0.3
Fe	0.8 ± 0.3	0.5 ± 0.3	0.5 ± 0.3
Na	0.5 ± 0.2	0.5 ± 0.2	0.6 ± 0.2
Total	3.1	2.4	2.0

** Impurity concentration listed as μg/gm.
*** Experiment duration was 4 hours.

II. – Powder Production

A total of 6.7 kg of silicon powder was produced in two separate experiments without opening the free-space reactor between experiments. The two experiments were conducted in series; between experiments, the powder was pneumatically transferred to the hopper of the melt-consolidation apparatus. After the second experiment, the powder pick-up tube

---

* Described in the previous Quarterly Report

plugged and the reactor was opened. No semi-solid growth formations were observed on either the gas injector or on the reactor wall.

In the first experiment of the above series, a silicon production rate of 2.8 kg/hr was maintained for one hour. It was estimated, from the exhaust flame color, that the pyrolysis efficiency was at least 95%. To exceed the 2.8 kg/hr production rate with the current reactor, minor modifications (e.g., replacement of low-flow regulating valves) would be required.

During the course of the 2.8 kg/hr experiment, the pressure inside of the reactor rose to 5 psig and remained at that level; the installation of a filter with a larger surface area will be required to control that pressure. The settling chamber of the reactor was designed to contain 7-10 kg of silicon powder. Consequently, for longer experiments at higher silane feed rates, continuous transfer to a larger storage vessel or consolidator will be required.

III. — Particle Growth

It was postulated that design modifications in the free-space reactor might produce particles over 1 μm in size. Indeed, modifications made to test this idea produced particles with an average calculated diameter of 1.3 μm.

The modifications consisted of injecting the silane gas upward from the bottom of the reactor and exhausting the gaseous hydrogen product through the top. This arrangement increased the residence time of the silicon powder in the reactor. With a wall temperature (center of the hot zone) of approximately 800°C, particles of average diameters ranging from 0.6 μm to 2.6 μm were obtained. The smallest particles (0.6 μm) were collected at the top of the reactor. Powder adhering to the reactor wall near the gas injector had an average size of 2.6 μm. The bulk of the powder collected from the settling chamber and its components had an average diameter of 1.3 μm. Through a water-sedimentation separation, non-spherical particles as large as 50 μm were identified.

2.2.2 SILICON CONSOLIDATION

During the present report period, construction and preliminary testing of the 152mm-diameter melt-consolidation apparatus were completed and the apparatus was attached to the free-space reactor. Powder transfer from the free-space reactor to the melter hopper was achieved in a semi-continuous operation, although some difficulties were experienced when only partial transfer occurred before the transfer line plugged. A variety of simple design modifications were attempted to resolve the problem but none was completely successful.

Free-space reactor powder that was pneumatically transferred to the hopper of the melter was intermittently melted between transfers. A total of 1.24 kg of silicon was melted at an average rate of 0.8 kg/hr (the powder actually melted as rapidly as it was fed into the quartz crucible). Slight degassing occurred during the melting operation and diminished between meltings. A small amount of dross (approximately 6.5mm wide) formed around the outer edge of the melt. This dross was analyzed and found to be silicon carbide. The most probable carbon source would be graphite-felt insulation used inside the melt consolidation apparatus. A high-purity quartz mat was ordered as replacement insulation. A 19mm-diameter rod that was suction-cast from the melt had an average electrical resistivity of 35 ohm-cm and p-type conductivity.

Powder from the same free-space experiment was melted in the melt-consolidation apparatus and vacuum-cast into a pellet as previously described; the conductivity type and resistivity were the same as those above.

2.3 CONCLUSIONS

Experiments were conducted in a quartz fluid-bed reactor to determine the operating modes required to obtain a spout-fluidized bed at room and elevated temperatures. The unpredictable nature of the gas-particle interactions made it necessary visually to observe bed characteristics. The condi-

tions for spout-fluidized beds at room temperatures were obtained. Insufficient experiments were conducted to specify the operating modes for spout-fluidized beds at elevated temperatures.

It was demonstrated that silane could be injected through a water-cooled gas inlet into a bed of hot silicon particles without forming deposits on the injector or on the reactor wall. The bed remained active throughout the experiment.

The formation of semi-solids in the free-space reactor are no longer considered road blocks for the continuous and long-term reactor operation. In an experiment that produced 6.7 kg of silicon powder, no semi-solids formed on either the injector or the reactor wall.

Most impurity sources within the free-space reactor — or those obtained through the handling of the fine powder — that could be identified through emission spectroscopic analysis were eliminated. The experiments indicate that the impurity level should fall below the limits detectable by our current techniques once the free-space reactor is operated for an extended period of time without dismantling. The melt consolidation apparatus attached to the free-space reactor will provide high-purity solid samples.

2.4 PROJECTED QUARTERLY ACTIVITIES

2.4.1 FLUID-BED REACTOR

- Improve the design and operation of the gas inlet system used in the silane pyrolysis reactor.

- Improve and evaluate safety features and procedures for the silane pyrolysis reactor.

- Evaluate the morphology of the silane pyrolysis product obtained under various feedstock, configuration, and operating conditions.

2.4.2 FREE-SPACE REACTOR

- Identify the critical factor for the pneumatic transfer of silicon powder.

- Generate engineering data for plant design and scale-up.

- Determine the effects of operating parameters on production rates.

2.4.3 SILICON CONSOLIDATION

- Optimize the powder-feed system of the melt consolidation apparatus.

- Determine the maximum combined feed and melting rate of the free-space reactor powder in the melt consolidation apparatus. Identify process limitation.

- Study powder compaction and sintering as a means for providing a feedstock source for the fluid-bed reactor and a marketable product.

3.0 PROCESS DESIGN

3.1 INTRODUCTION

The purpose of this program, started in October 1977, is to provide JPL with engineering and economic parameters for an experimental facility capable of producing 25 metric tons of silicon per year by the pyrolysis of silane gas. An ancillary purpose is to estimate the cost of silicon produced by the same process on a scale of 1000 metric tons per year.

Preliminary process specifications have been formulated, and all process design efforts are based on these specifications. In the silane production process, two processing schemes are being evaluated; the evaluation includes material balance, column design, and other work necessary to judge the relative merits of the two process arrangements. The preferred processing scheme will be selected in early January.

The preliminary block flow diagram is complete, including heat and mass balance for all battery-limit streams. The preliminary process flow diagram and the heat and mass balance for all internal streams of the silane process are nearing completion. The preliminary distillation column design has been made.

Some key process design data are missing for reliable heat and mass balance work. A program for acquiring these data will be outlined shortly.

3.2 DISCUSSION

3.2.1 PROCESS DESIGN PHILOSOPHY

Although the silane plant and the pyrolysis/consolidation plant are fairly independent, the process design will be based on an integrated plant concept. It is assumed that this plant will accept metallurgical-grade silicon and will produce solar-grade silicon shots or rods on a continuous basis. It was decided that hydrogen will not be recycled from the pyrolysis reactor to the hydrogenation reactor in the experimental 25 MT/yr facility.

3.2.2 PRELIMINARY PROCESS SPECIFICATIONS

Based on available process design data from Parma, Sistersville, and Tarrytown, key process specifications have been assembled.(3.1) The process parameters, some of which will be presented below, will form the basis of the preliminary process design of a 25 MT/yr experimental facility. Missing specifications will be prepared as additional process data become available.

Plant Capacity. The experimental facility will produce 25 MT/yr of solar-grade silicon and it is assumed that it will be on-stream 63% of the year. The following flow rates will be used:

Metallurgical Grade Silicon	13.0 lb/hr
Hydrogen to Hydrogenation Reactor	1.5 lb/hr
Hydrogen Chloride to Hydrogenation Reactor	make-up
Copper Powder Catalyst	make-up
Silane to Pyrolysis Reactor	12.0 lb/hr
High-Purity Silicon Product	10.0 lb/hr
Hydrogen Effluent from Pyrolysis Reactor	1.5 lb/hr
Silicon Powder Loss	0.5 lb/hr

Hydrogenation. Hydrogenation of silicon tetrachloride is carried out in a fluid-bed reactor and is represented by the following equation.

$$3SiCl_4 + 2H_2 + Si(M\text{-}G) \underset{}{\overset{Cu}{\rightleftharpoons}} 4HSiCl_3$$

Hydrogenation Reactor	fluid bed
Temperature	500°C
Pressure	300 to 500 psig
Mean Particle Diameter of Silicon	150 μm

Fluidization Velocity	0.2 to 0.3 ft/sec
Gas Residence Time in Bed	15 to 20 seconds
Catalyst	Copper
Catalyst/Si (M-G) Feed Ratio	1 to 20%

Trichlorosilane Redistribution. The redistribution of TCS into dichlorosilane and STC is effected in the presence of an ion-exchange catalyst.(3.2) The reaction is represented by:

$$2HSiCl_3 \underset{\longleftarrow}{\xrightarrow{\text{catalyst}}} H_2SiCl_2 + SiCl_4$$

Redistribution Reactor	packed bed
Temperature	80°C
Pressure	(50 psig)
Fluid State	liquid
Residence Time	360 seconds
Catalyst	Amberlyst A-21 resin

The desirable operating pressure has not yet been determined.

Dichlorosilane Redistribution. The redistribution of dichlorosilane to produce silane and TCS is carried out over the amine catalyst according to the following equations:

$$4H_2SiCl_2 \rightleftharpoons 2H_3SiCl + 2HSiCl_3$$

$$2H_3SiCl \rightleftharpoons SiH_4 + H_2SiCl_2$$

The net reaction is:

$$3H_2SiCl_2 \overset{\text{catalyst}}{\rightleftharpoons} SiH_4 + 2HSiCl_3$$

Redistribution Reactor	packed bed
Temperature	55°C
Pressure	(40 psig)
Fluid State	vapor
Residence Time	10 seconds
Catalyst	Amberlyst A-21 resin

Silane Purity. In order to attain the desired purity for the silicon product, silane fed to the pyrolysis reactor must meet the following purity requirements:

Phosphorous	1 ppb
Boron	0.3 ppb
Iron, heavy metals	1 ppb
Carbon	(5 ppb)
Chlorosilanes	(20 ppm)
Nitrogen	500 ppm
Hydrogen	1%
Moisture	-80°C dew point

Because carbon and chlorosilane levels are uncertain, realistic values will be assigned later.

3.2.3 EVALUATION OF TWO SILANE PROCESS SCHEMES

Two silane production schemes are under consideration. The Adsorption Silane Process (ASP) given in Figure 3.1 most closely resembles the process adopted for the PDU facility built at Sistersville. It uses a combination of redistribution reactors and distillation columns to yield a 97% pure silane stream, which is then purified to specifications using a carbon adsorber. The second schematic, called the Distillation Silane Process (DSP) shown in Figure 3.2, replaces the adsorber with additional distillation and redistribution. The two schemes are identical in the hydrogenation step and differ only after the production of the crude TCS/STC mixture.

An equipment comparison of the two schemes in a 1000 MT/yr commercial plant shows that DSP requires more equipment but the equipment is generally smaller than that for ASP. Capital costs are expected to be approximately equal, with the possibility that costs for DSP would be slightly higher.

Operating costs indicate that utility costs will be somewhat higher for ASP due to greater anticipated refluxing requirements of the second distillation column and to temperature cycling in the carbon adsorber. Uncertainty is introduced

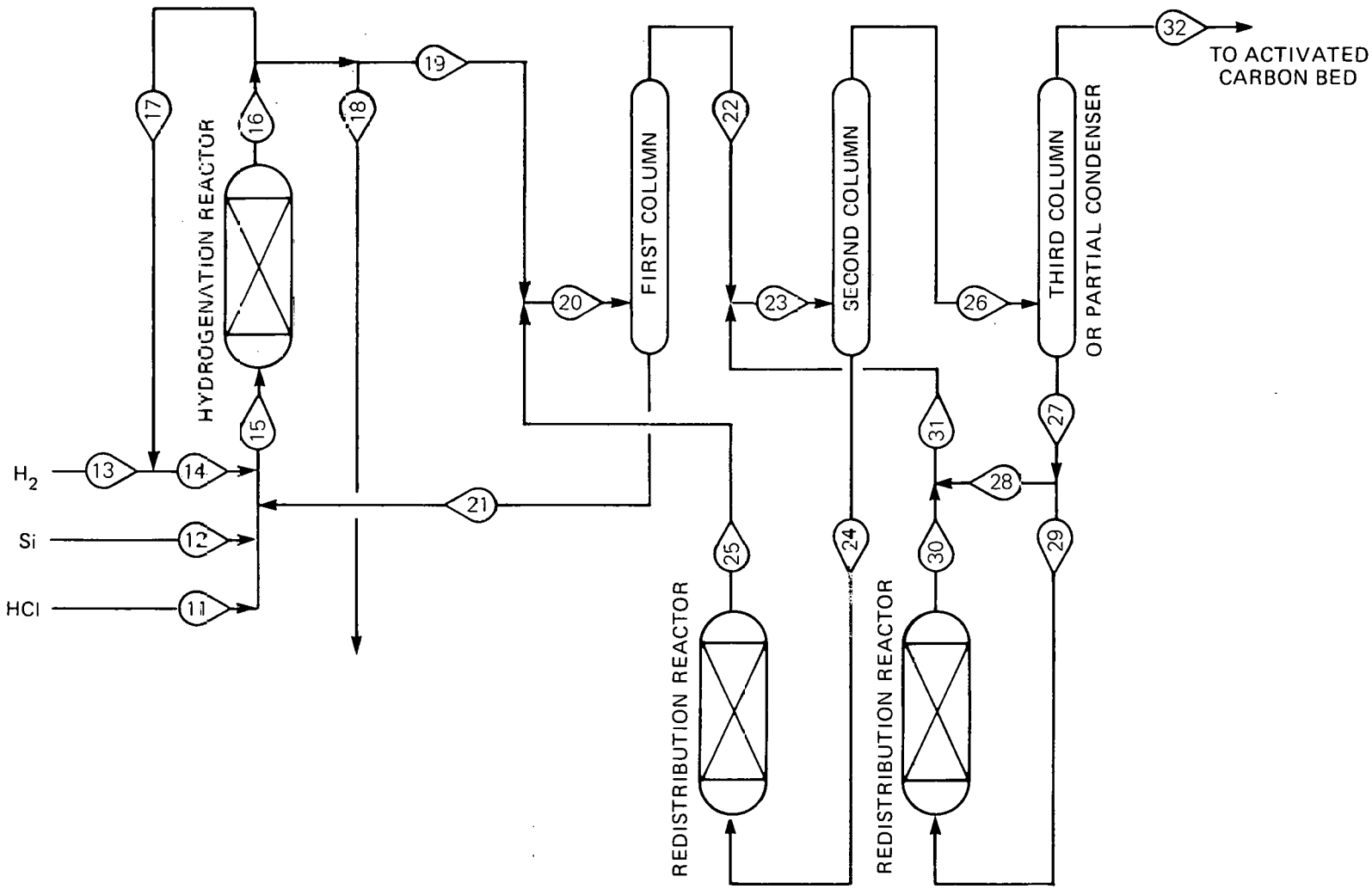

Figure 3.1
ADSORPTION SILANE PROCESS FOR ULTRA-PURE SILANE PRODUCTION

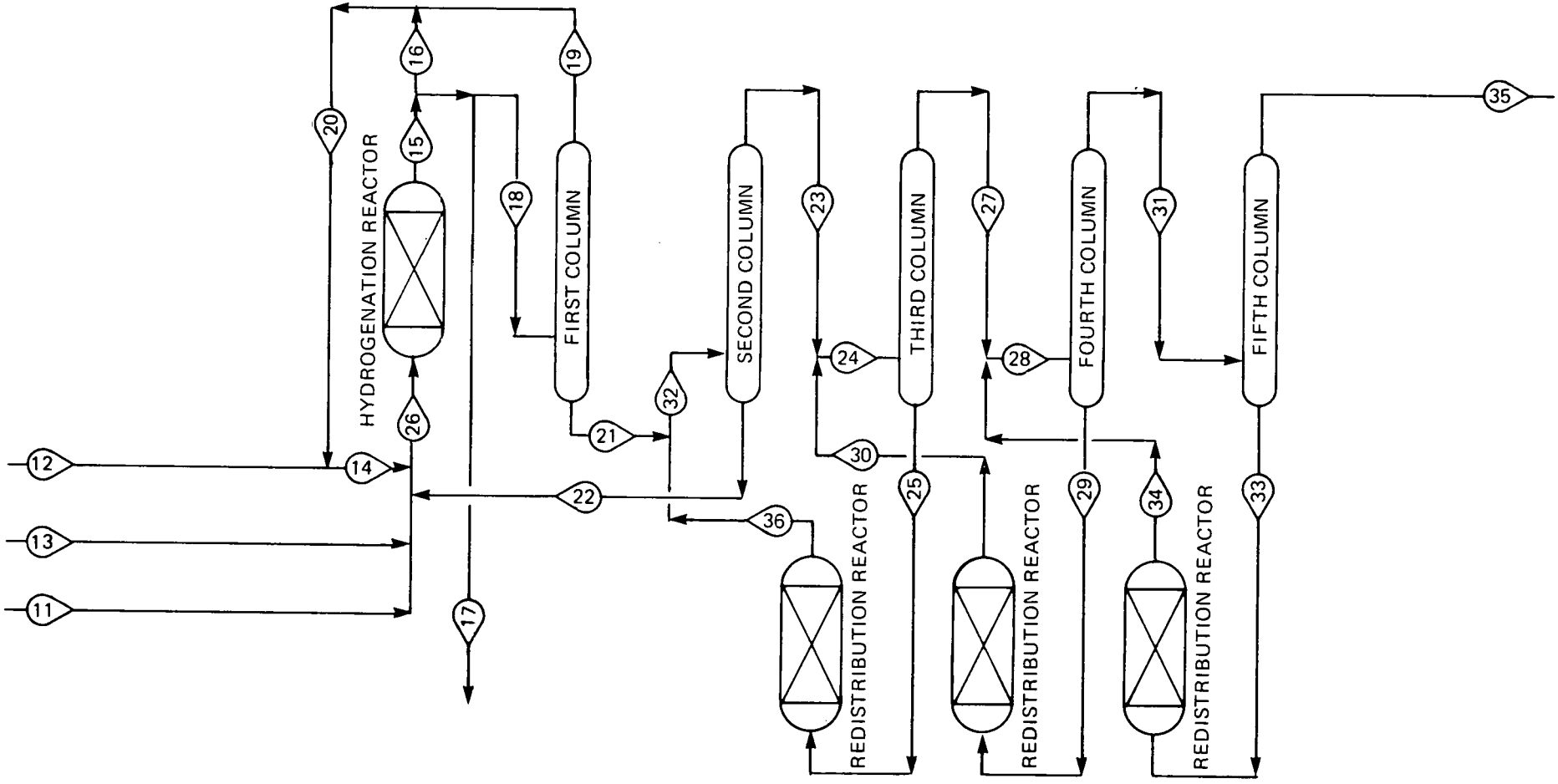

Figure 3.2
DISTILLATION SILANE PROCESS FOR ULTRA-PURE SILANE PRODUCTION

into the utility consumption of the ASP scheme because of insufficient data for accurately sizing the adsorber regeneration recycle stream.

Process uncertainties seem slightly to favor the DSP scheme. If the desired chlorosilane levels are not met by constructing to a certain design, the levels can be adjusted easier in the DSP scheme. However, if certain light components, such as HCl, were produced in the process, ASP could handle them easier. Plugging of the carbon bed by metal hydrides could be a problem with adsorbers, since they operate in the gas phase at low velocity. Distillation equipment is likely to stay cleaner because the surfaces are constantly flushed with liquids and the velocities are higher. DSP will produce silane of consistent quality while ASP may yield some transient impurities as adsorber beds are switched for regeneration. Valve leakage around the adsorbers could be very damaging to silane purity — a potential difficulty eliminated by the DSP scheme. The preferred scheme will be chosen in January.

3.2.4 PARAMETRIC STUDY

3.2.4a HYDROGENATION REACTOR

A scoping study has been completed (3.3) to assess the relative economic impact of hydrogen/STC feed ratio and operating pressure on the hydrogenation reactor and related equipment. The study is based on a 1000 MT/yr commercial size

plant but is pertinent to the 25 MT/yr experimental facility as well.

At the time the study was performed, the process scheme was incomplete, and various assumptions had to be made concerning downstream conditions and equipment. Only three cases were examined: (1) $H_2/SiCl_4$ = 1.5 moles/mole and pressure = 200 psig; (2) $H_2/SiCl_4$ = 2.0 and p = 200 psig; and (3) $H_2/SiCl_4$ = 1.5 and p = 500 psig. We realize that the evaluation of these three cases will not be sufficient to select the optimum ratio and pressure. However, trends and relative impact of parameters on equipment and utility cost can be estimated.

The study indicates that a $H_2/SiCl_4$ ratio in the range of 1-2 does not seriously affect equipment cost. A lower ratio gives only about 4% lower utility cost than does a higher ratio. It is safe to say that, in the range examined, the $H_2/SiCl_4$ ratio should be selected for process rather than economic considerations.

The hydrogenation pressure plays a major role in plant economics. Increasing the pressure from 200 to 500 reduces the equipment cost by 25% and the power cost by 10%. Further increase in reactor pressure may be beneficial, but other factors such as equipment availability, fabrication details, and safety must all be considered.

3.2.4b DISTILLATION COLUMN

A brief parametric study was conducted to define the most likely range of distillation operating pressures on the basis of process feasibility and economics. Work is based on the preliminary computer mass balance of the Distillation Silane Process. The assumption is made that the separation difficulty is only a function of light and heavy keys so that a McCabe-Thiele approach can be used.

An in-house distillation design computer program (MDCC) was used to examine every column under various pressures and reflux ratios. When a column has two feeds, they were brought in at the optimum tray location. Columns, condensers, refrigeration, and reboilers were sized and costed. Cases were compared for capital and operating cost.

This brief study indicates that the most favorable pressures appear to be 35-50 psig for the TCS/STC column and 300-400 psig for the other columns. For the conservative design, surface tension will limit the pressures to 340, 370, and 400 psig in the last three columns. All comparative parametric studies for purposes of process arrangement and operating condition optimization have been based on the commercial 1000 MT/yr facility.

3.2.5 HEAT AND MASS BALANCE

3.2.5a REDISTRIBUTION EQUILIBRIUM

Redistribution steps in the silane production involve the simultaneous equilibrium of the following reactions:

$$2HSiCl_3 \rightleftharpoons H_2SiCl_2 + SiCl_4$$

$$2H_2SiCl_2 \rightleftharpoons H_3SiCl + HSiCl_3$$

$$2H_2SiCl \rightleftharpoons SiH_4 + H_2SiCl_2 \quad (3.4)$$

A Fortran subroutine was developed[3.4] for accurately and efficiently calculating the equilibrium composition of a flow stream in which the above reactions are simultaneously occurring. Inputs to the program are the equilibrium constant for each reaction and the Cl/Si mole ratio; outputs are the equilibrium mole fraction of $HSiCl_3$, H_2SiCl_2, H_3SiCl, SiH_4 and $SiCl_4$.

3.2.5b PRELIMINARY BLOCK FLOW DIAGRAM

A set of computer subroutines were written to perform a battery-limit heat and mass balance of the 25 MT/yr experimental facility. Work was carried out on both the Adsorption Silane/Silicon Process and the Distillation Silane/Silicon Process at two hydrogenation pressures of 300 and 500 psig. In

each case the process was grouped into three blocks or sections. Section 1 is the hydrogenation section, Section 2 is the fractionation and redistribution, and Section 3 contains the silane pyrolysis and silicon consolidation.

The initial phase of the work was completed and documented. (3.5) The computer output includes the following:

- Stream Catalog — giving all battery-limit stream numbers, their descriptions, temperatures and pressures.

- Stream Heat and Mass Balance Table — listing all stream components and their flow rates. It also shows the elemental composition, pressure, temperature, liquid fraction, enthalpy, average molecular weight, and other physical properties. This type of table is produced for all battery-limit streams.

- Section Heat and Mass Balance Tables — One table gives the heat balance around a section and the overall heat imbalance. Another table presents the mass balance around the section and the overall mass imbalance.

- Overall Heat and Mass Balance Tables — giving heat and mass balance for the overall silicon/silane process.

The block flow diagram will be updated as required.

3.2.5c PRELIMINARY MASS BALANCE FOR SILANE PRODUCTION

A set of computer programs has been written to compute a mass flow rate for every stream of the silane process (Figures 3.1 and 3.2), and a heat balance for every stream will be added.

The hydrogenation and redistribution reactions were assumed to take place according to reactor operating conditions presented earlier. The redistribution computer program discussed in Section 3.2.5a was used to compute all redistribution product streams. All distillation columns were assumed to yield 97% recovery, except those columns noted below.

The preliminary mass balance for a 25 MT/yr capacity was performed on two silane processes, Adsorption Silane Process and Distillation Silane Process, both at 500 psig hydrogenation pressure. ASP assumes that the separator (Column 3 in Figure 3.1) performs in the following manner:

- 97% silane recovery,
- 0.79% monochlorosilane recovery,
- 0.04% dichlorosilane recovery.

DSP assumes that Column 5 recovers silane 100%. The mass balance around each column will give a good starting point for the next step. A special in-house computer program (MDCC) employs the first-cut mass balance around the column as the input and then optimizes the column design. The column design of the Distillation Silane Process is two-thirds completed. The thermodynamic data, such as vapor pressure and enthalpy, for silane, silicon tetrachloride, and the three chlorosilanes were prepared in a form suitable for the MDCC program. Process designs for the first three columns have been completed. Figure 3.3 shows the DSP schematic and specifies the total flow, temperature, and pressure of every stream as well as the numbers of trays needed in the distillation column.

3.2.6 CONCEPTUAL DESIGN

3.2.6a HYDROGENATION REACTOR

Conceptual design work was performed on the hydrogenation reactor and on the pneumatic feed system for introducing powdered metallurgical-grade silicon into the reactor. A single-lock hopper and a fluidized feeder vessel are proposed for the feed system. Metallurgical-grade silicon (98-99% pure) is charged into the lock hopper, purged with

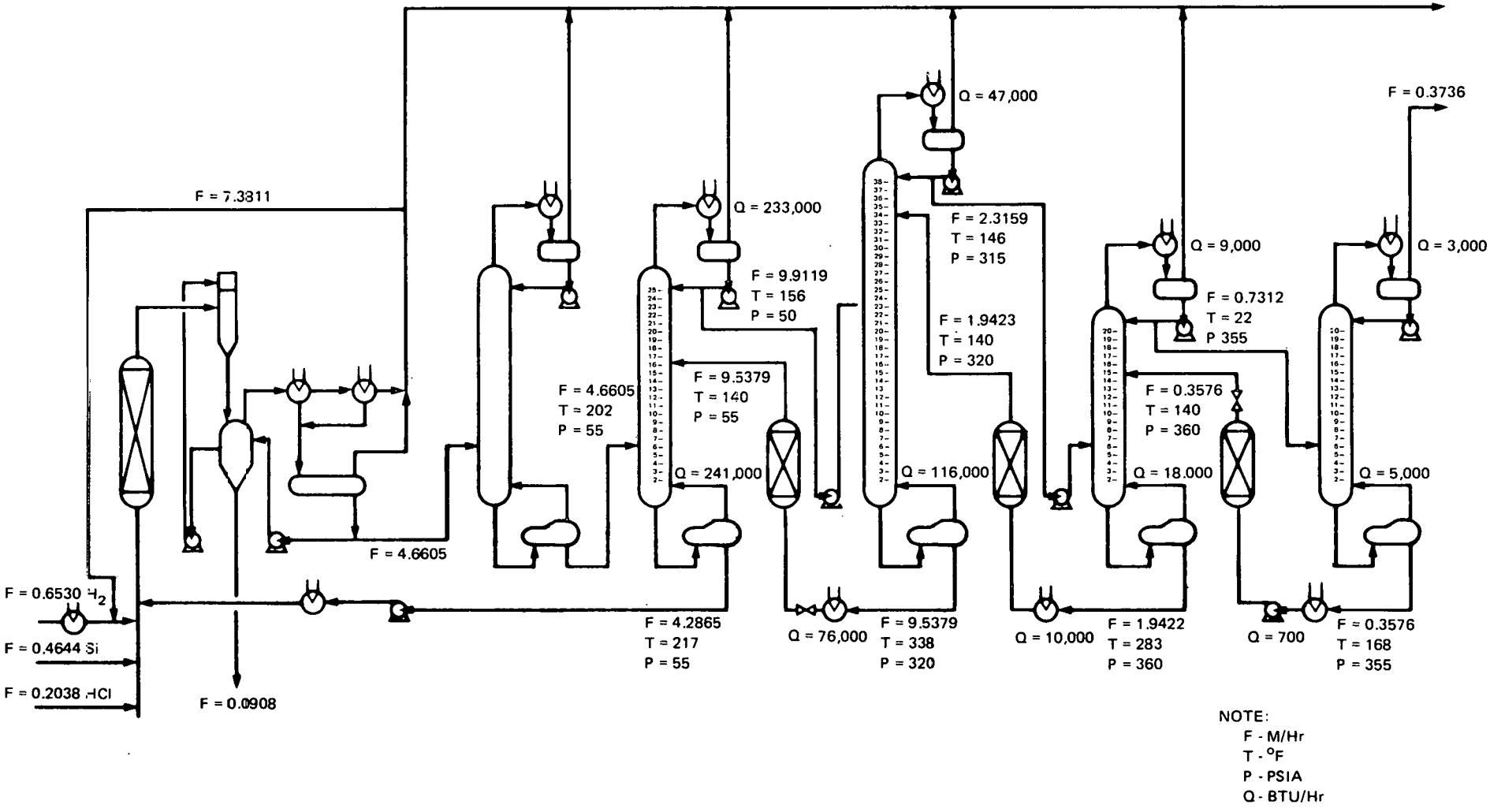

Figure 3.3
THE DISTILLATION SILANE PROCESS SCHEMATIC

nitrogen to eliminate atmospheric contaminants, pressurized, and finally discharged into the fluidized feeder vessel. The feeder vessel provides the required feed of powdered silicon to the reactor using hydrogen as the transport gas. For the 25 MT/yr plant, the reactor consists of an 8" N.S. stainless-steel pipe with an expanded section at the top to minimize elutriation.

3.2.6b PYROLYSIS SYSTEM

Work was started on the process design for silane pyrolysis and silicon consolidation. Conceptual work on an integrated free-space pyrolysis/consolidation system is underway.

3.2.7 PROCESS DESIGN DATA STUDY

Process design calculations for the 25 MT/yr experimental facility were initiated. We believe that the proposed processes will produce ultra-high-purity silane and thus semiconductor-grade silicon, by applying conventional unit operations of distillation, redistribution, and pyrolysis. However, assembly of a reliable design requires additional data.

To assist in identifying these data, the correlations used in the PROBE process simulation computer system were studied. For every data point, correlations, computational procedures, and data source (if available) were examined and documented. (3.6)

Although a final list of necessary data for reliable heat and mass balance work will not be completed until mid-January, preliminary identifying work was accomplished and documented in December, (3.7) as briefly summarized below:

1. Equilibrium data, and additional kinetic data are required for Amberlyst A-21-catalyzed disproportionation of three chlorosilanes (trichloro-, dichloro-, and monochloro- silanes).

2. Vapor-liquid equilibrium data are required for mixtures containing $SiCl_4$, SiH_4, and the three chlorosilanes. Vapor pressure data are available, but non-ideality data are not.

3. Solubility and vapor-liquid equilibrium data in chlorosilanes are needed for all contaminant metal chlorides and hydrides appearing in the system. This information will permit the assembly of a process design for their rejection and the ultimate production of high-purity silane.

4. Neither a mechanism nor kinetics for the high-temperature, fluidized bed hydrogenation

of $SiCl_4$ has been suggested or measured. A modeling effort hypothesizing a reaction mechanism and defining kinetic expressions is needed.

The availability of the above-defined process design data will substantially increase our ability to design a silicon production facility capable of meeting or exceeding capacity and purity goals.

3.2.8 EQUIPMENT VENDOR SEARCH

Based on the preliminary silane/silicon process design, a vendor equipment list was compiled and every piece of equipment was roughly sized. Vendor contacts have been initiated.

3.3 CONCLUSIONS

Based on the available process design data, key process specifications were assembled. These will form the basis for the preliminary process design of a 25 MT/yr experimental facility.

Two silane production schemes are under consideration and in early January a decision will be made regarding the preferred process scheme. All future work will then be based on the selected scheme.

A scoping study was completed to assess the relative economic impact of hydrogen/STC feed ratio and operating pressure on the hydrogenation reactor and related equipment. The study indicates that the $H_2/SiCl_4$ ratio in the range of 1-2 does not seriously affect the equipment. The hydrogenation pressure plays a major role in plant economics. Increasing the pressure from 200 to 500 psig reduces equipment cost by 25% and power cost by 10%.

A similar study was conducted on the most likely range of distillation operating pressure. Desirable pressures appear to be 35-50 psig for the TCS/STC column and 300-400 psig for the other columns. All comparative parametric studies have been based on a commercial 1000 MT/yr facility but are pertinent to the 25 MT/yr experimental facility as well.

The initial phase of a battery-limit heat and mass balance was completed. The mass balance of all streams of the silane process is almost complete.

Conceptual designs for the hydrogenation reactor and/or the integrated free-space pyrolysis/consolidation systems are underway.

3.4 PROJECTED QUARTERLY ACTIVITIES

3.4.1 PROCESS DESIGN OF THE 25 MT/YR EXPERIMENTAL FACILITY

Preliminary heat and mass balance for all streams, all equipment preliminary functional specifications, a plant layout, and a process flow diagram will be completed. Based on the above, a preliminary process design package for the 25 MT/yr experimental facility will be prepared. Process design work on the fluid-bed pyrolysis and the 1000 MT/yr commercial plant will commence.

3.4.2 PROCESS DESIGN DATA ACQUISITION

A list of required data will be finalized and a program for their acquisition will be outlined; the program cost will be estimated and work will be initiated.

3.4.3 ECONOMIC ANALYSIS

Based on the preliminary process design, all equipment will be costed for the 25 MT/yr facility. Major equipment for the 1000 MT/yr plant will also be estimated. Preliminary utility investment, plant cost, and operating cost for the experimental facility will be prepared.

3.5 REFERENCES

3.1 S. K. Iya, "Preliminary Process Design of 25 MT/yr Experimental Facility: Process Specification", Engineering Memorandum No. 6150, (SGS-1), Linde Division, Union Carbide Corporation, Tonawanda, New York, November 18, 1977.

3.2 W. C. Breneman and J. Y. P. Mui, Project Report File No. SVP-77-13, Union Carbide Corporation, Sistersville, West Virginia, February 1, 1977.

3.3 L. M. Coleman, "Hydrogenation Reactor Parametric Study", Engineering Memorandum No. 6155 (SGS-2), Linde Division, Union Carbide Corporation, Tonawanda, New York, December 9, 1977.

3.4 L. D. Potts, "A Computer Subroutine for Chemical Flow Equilibrium in Mixtures of Chlorinated Silanes", Engineering Memorandum No. 6152 (SGS-3), Linde Division, Union Carbide Corporation, Tonawanda, New York, December 1, 1977.

3.5 T. E. Diegelman, "Integrated Heat and Mass Balance for 25 MT/yr Block Flow Diagram", Engineering Memorandum No. 6158 (SGS-4), Linde Division, Union Carbide Corporation, Tonawanda, New York, December 9, 1977.

3.6 T. E. Diegelman, Intradepartmental Memorandum to E. Buck, December 27, 1977.

3.7 R. A. Beddome, "Process Design Data Needs for High-Purity Silane Production", Engineering Memorandum No. 6159 (SGS-5), Linde Division, Union Carbide Corporation, Tonawanda, New York, December 14, 1977.

3.8 D. R. Stull and A. Prophet, "JANAF Thermodynamic Tables", Second Edition, U. S. Department of Commerce, NBS, July, 1977.

3.9 E. O. Brim, "Thermodynamic Data on the Reaction of Silicon Tetrachloride with Hydrogen and Trichlorosilane in the Presence of Silicon Metal", Silicon Metals Process Development Memorandum No. C-49, Linde Division, Union Carbide Corporation, Tonawanda, New York, July 1, 1948.

4.0 CAPACITIVE FLUID-BED HEATING

4.1 INTRODUCTION

This program will explore the feasibility of utilizing electrical capacitive heating to control fluidized silicon bed temperature during the heterogeneous decomposition of silane.

Both steel-wall and glass-wall reactors have been fabricated and assembled. The first series of short experiments in the steel-wall reactor produced a silicon-bed temperature of over 100°C, indicating that fluidized particles can be heated by high-frequency capacitive heating. As the bed temperature was increased a sudden, unexplained drop in bed impedance at 32°C was observed. The impedance drop was relatively independent of frequency. A multi-tap matching transformer was ordered to compensate for the low bed impedance. Tests in the glass-wall reactor have just begun; this reactor allows us to observe bed behavior along with chemical and physical surface changes. Heating tests were also conducted with a ceramic-coated electrode. The electrode maintained its integrity throughout the frequency range tested.

4.2 DISCUSSION

4.2.1 THEORETICAL MODEL

The model we developed is divided into three parts. The first part is an analysis of silicon deposition

from a gas stream onto a flat surface. The second part involves determining the conditions under which this deposition occurs in a stable manner and without homogeneous decomposition. The third part applies the above findings to a three-dimensional model, i.e., finding the concentration and temperature profiles in the emulsion phase of the fluid-bed.

The first part, describing the deposition rate occurring on a flat surface, has been discussed before.[4.1,4.2] The model developed here is similar, except that thermal conductivity and diffusion coefficient are assumed to be temperature dependent.[4.2] Since the layer over which the deposition occurs has a very large temperature gradient, we believe that the temperature dependency of these properties needs to be incorporated.

The general equation for heat and mass transfer across a thin layer can be solved if relatively simple temperature dependencies for the diffusion coefficient and thermal conductivity are assumed. It turns out that both are very well represented at temperatures of interest as power laws[4.3,4.4], with $k \propto T^{0.75}$, and $D \propto T^{1.75}$. These allow analytical solution of the equations with proper boundary conditions, though the results are more complicated than in the case of constant coefficients.

The other important element in this analysis is the reaction rate at the surface of the substrate. There is wide disagreement in the literature on this point, and it has been pointed out [4.2] that even careful analysis does not provide information on the underlying physical mechanisms. For our analysis, the results of Everstein and Put [4.5] are used because they are given in functional form and seem physically reasonable.

It is an observed experimental fact that when the silane concentration exceeds a certain level at a given temperature, homogeneous decomposition occurs. One group of researchers [4.1] found that this critical concentration could be expressed by an Arrhenius relation. If this result is accepted, one can determine if the critical concentration is exceeded at any point in a thin layer. It has also been possible to determine the conditions (as a function of gas-stream silane concentration and of gas and substrate temperatures) under which no homogeneous decomposition occurs in the layer.

As a final step, the developed heat and mass transfer relations and stability criteria were applied to the conditions existing in the emulsion phase of the fluid-bed. This determines the maximum allowable inlet silane concentration into the bed, the required path length through the emulsion phase, and the effects of varying bed parameters.

It is worthwhile to note that in almost all cases of interest (save at very high temperatures or with very large particles) the reaction in the emulsion phase of a fluid-bed should be reaction-rate controlled and not diffusion controlled. Thus, the model used here is an extension of that in Reference 4.6 to include finite reaction rate.

At a given bed condition, the silane pyrolysis is either reaction-limited or diffusion-limited. Reactor volume and stability depend on the regime in which the bed will be operating. When pyrolysis is diffusion-limited, silane tends to decompose in a free space, away from the bed particles. Figure 4.1 plots the boundary between the two regimes employing particle diameter and temperature as parameters.

The model was incorporated into a computer program to determine the regimes of stability (heterogeneous decomposition) for the fluid-bed reactor. It will also be used to predict conversion efficiency and to optimize key design parameters by relating heat-exchange duty, reactor size, throughput, and particle diameter.

4.2.2 TESTING WITH STEEL WALL REACTOR

Construction of the steel reactor system shown in Figure 4.2 was completed, and debugging tests were started. The first series of short experiments produced a bed temperature

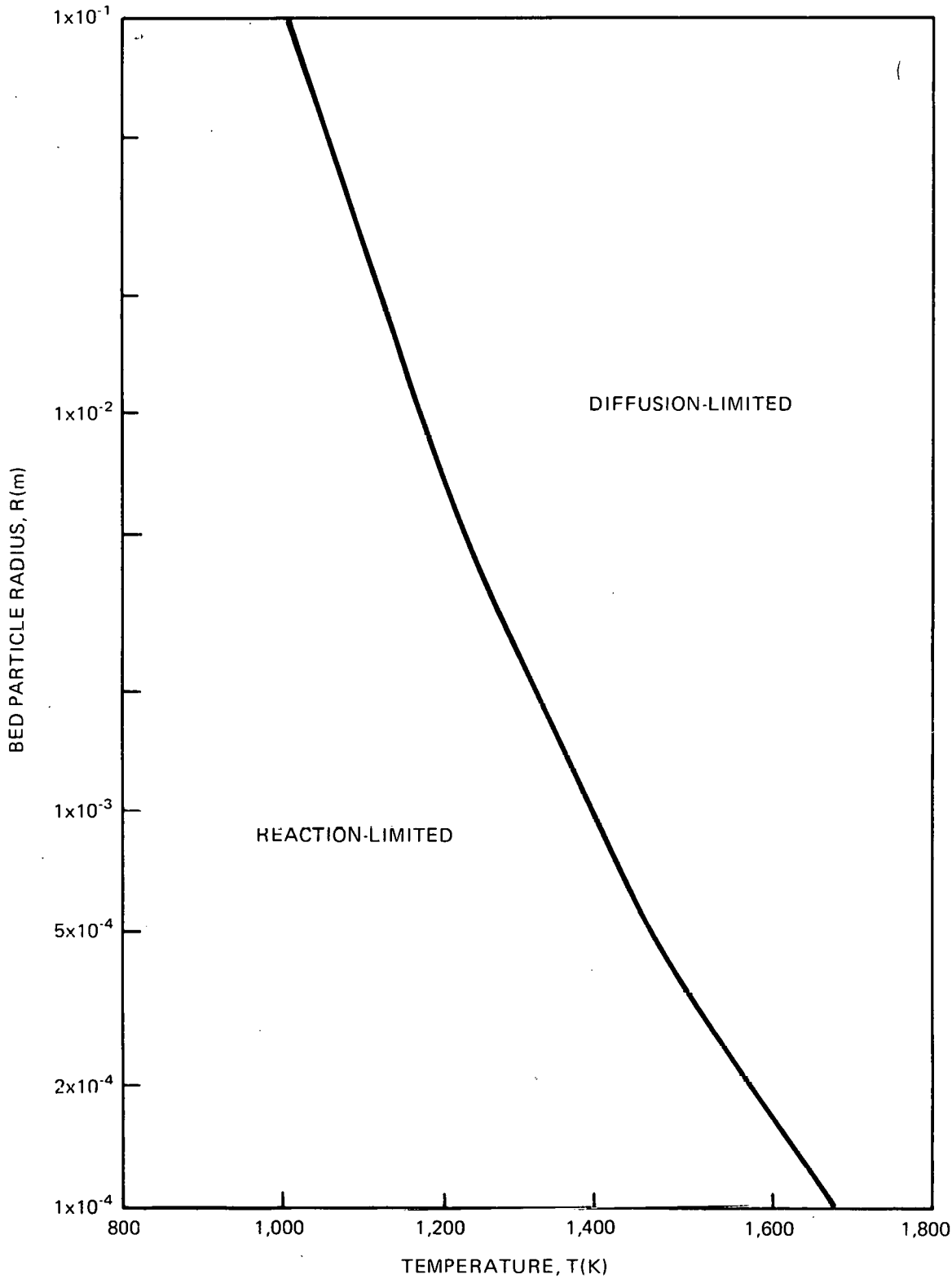

Figure 4.1
REACTION-LIMITED AND DIFFUSION-LIMITED REGIMES

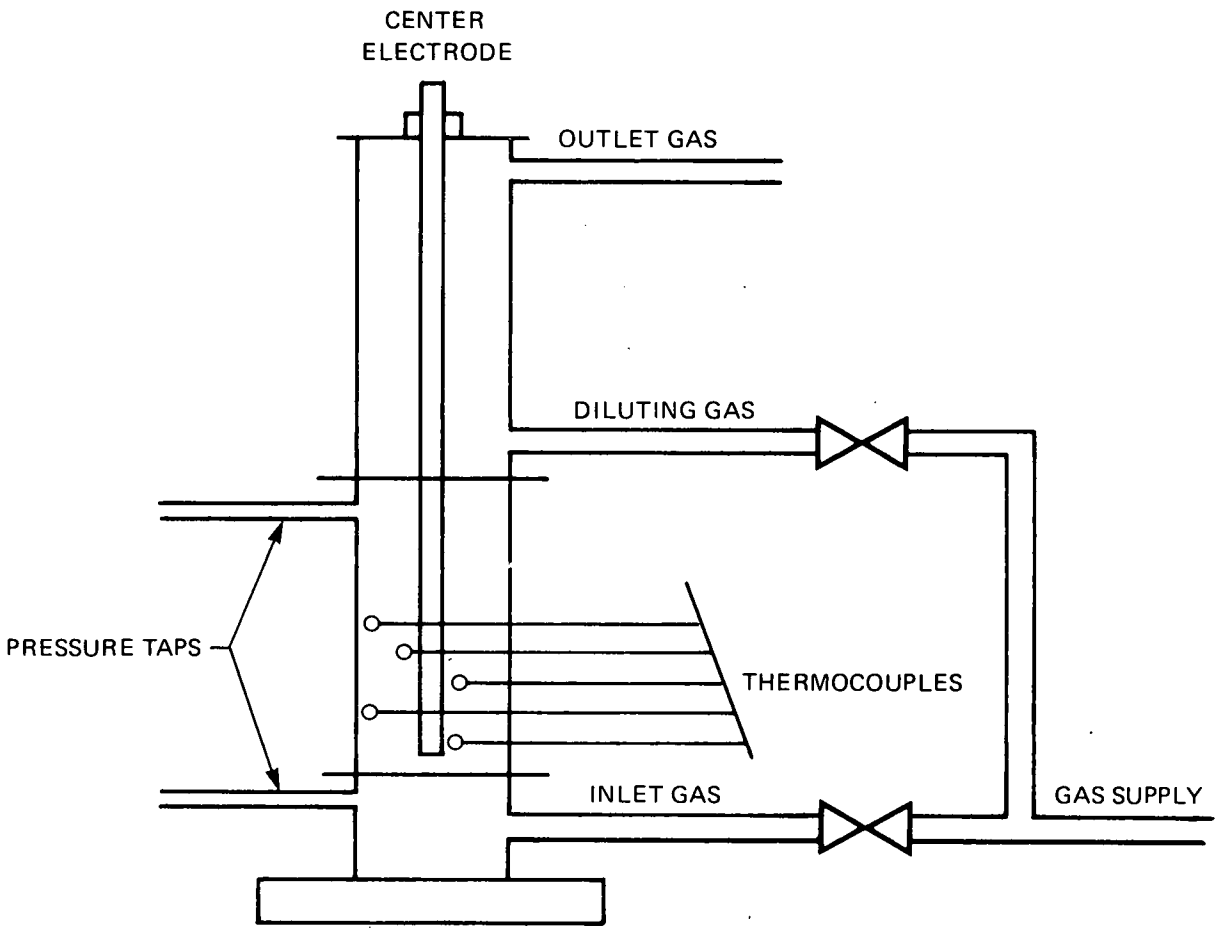

Figure 4.2
STEEL WALL REACTOR

in excess of 100°C, indicated that fluidized particles can be heated by high-frequency capacitive heating. Metallurgical-grade silicon was used as bed particles in these tests.

Initially, the bed had a relatively high resistance that was strongly frequency-dependent ($R \simeq 100\,\Omega$ at f = 10 MHz; $R > 1000\,\Omega$ at f = 500 kHz). This mode of behavior persisted until the temperature reached approximately 32°C, when a sudden drop in resistance occurred. The impedance dropped approximately to $10\,\Omega$, and the drop was largely independent of frequency. The drop was sudden in every case, occurring as a sharp transition between the two states with approximately a one-minute period in which the bed appeared to jump back and forth from one state to another. This behavior is unexplained at this time. We plan to repeat the experiment using argon as the fluidizing gas instead of nitrogen.

4.2.3 TESTING WITH GLASS WALL REACTOR

The glass-wall reactor system shown in Figures 4.3 and 4.4 was assembled and tests have begun. As with the metal-wall reactor, we were able to heat the bed in the fluidized state. A rough heat balance shows that the electrical power into the bed mostly goes into the fluidizing gas with some heat loss through the reactor wall.

The glass-wall reactor enables us to observe the behavior of the bed. In general, a normal quality of fluidiza-

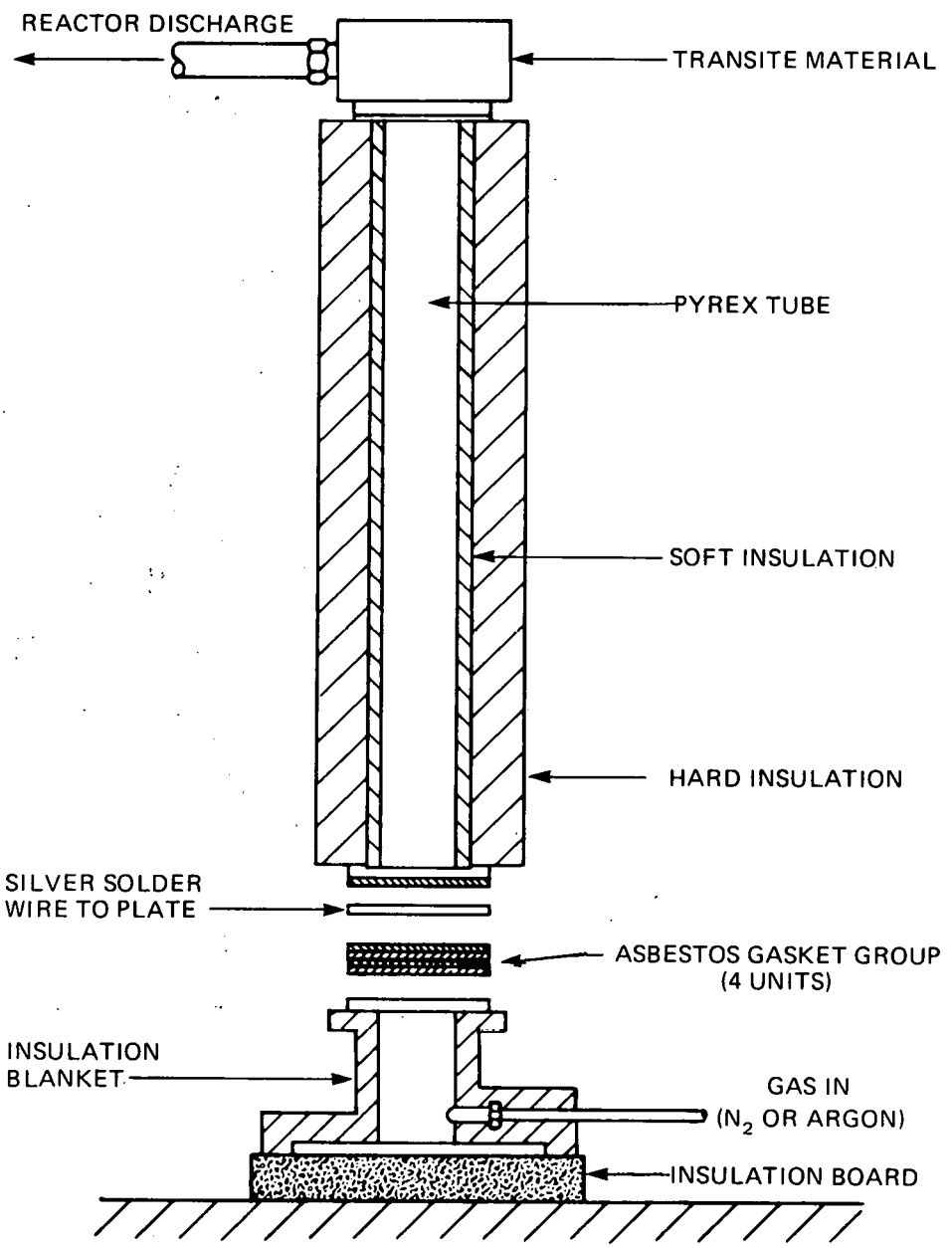

Figure 4.3
GLASS WALL REACTOR DESIGN

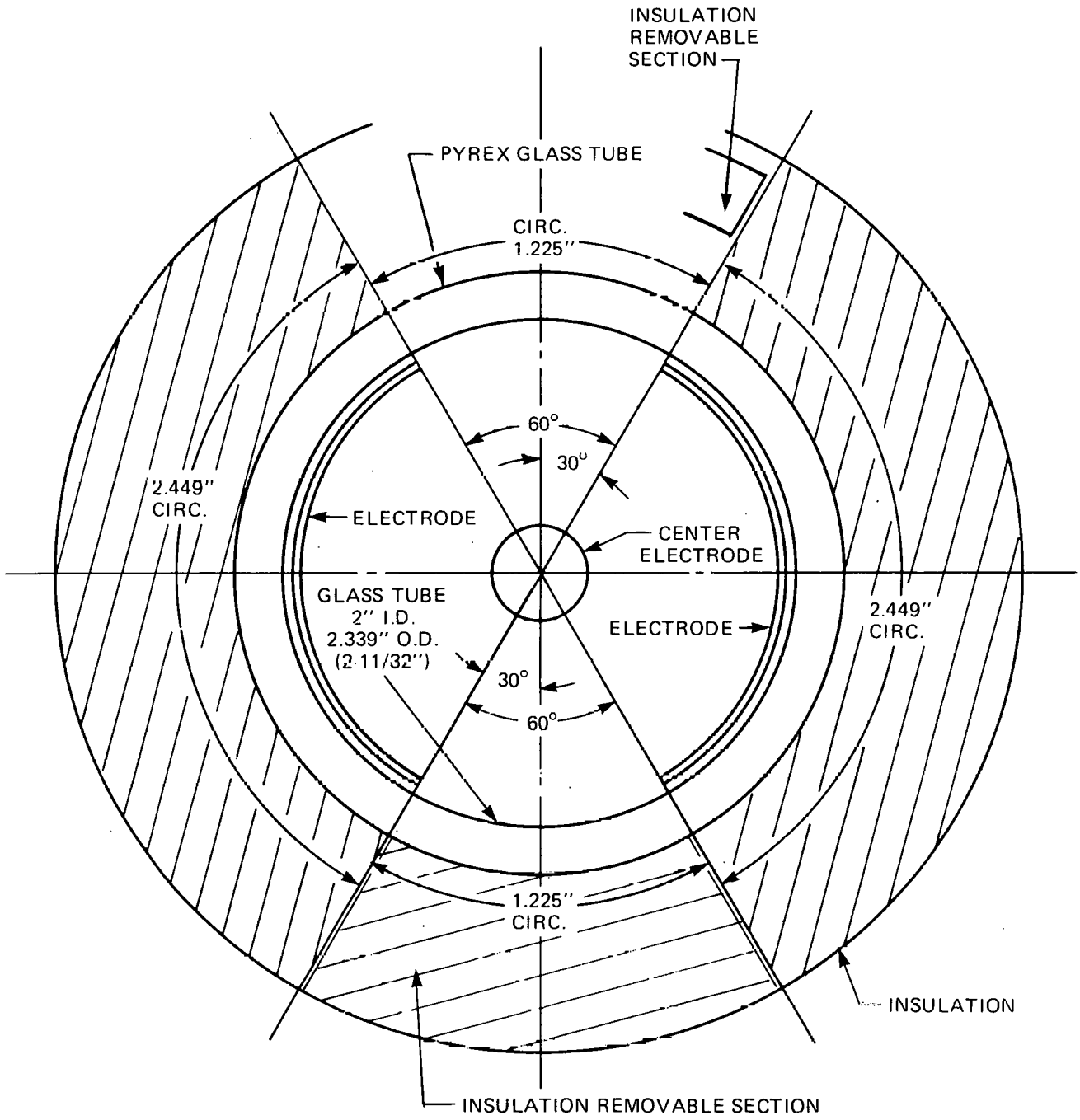

Figure 4.4
GLASS WALL REACTOR CROSS SECTION

tion was attained without any anomalous tendency such as slugging or channelling. The particles used in this series of tests were -20/+40 mesh, metallurgical-grade Alfa silicon.

More quantitative experiments will be conducted to measure fluidization parameters and to study surface physical and chemical changes during heating.

4.2.4 TESTING WITH COATED ELECTRODE

The center electrode was coated with a commercial ceramic cement as shown in Figure 4.5. Tests with the ceramic-coated electrode show that the coating maintains its electrical integrity throughout, as shown by the measured current through the bed; the current vanishes at low frequencies. The measured voltage/current relationship is given in Figure 4.6.

It is expected that the addition of a coating on the outer electrode will add a larger additional capacitance in series with the rest of the circuit. Additional capacitance implies a higher frequency requirement for bed heating. Eventually, the electrodes will have to be coated with silicon or silica to avoid contamination. We do not plan to coat the outer electrode since no changes to the circuit, other than capacitance, are expected.

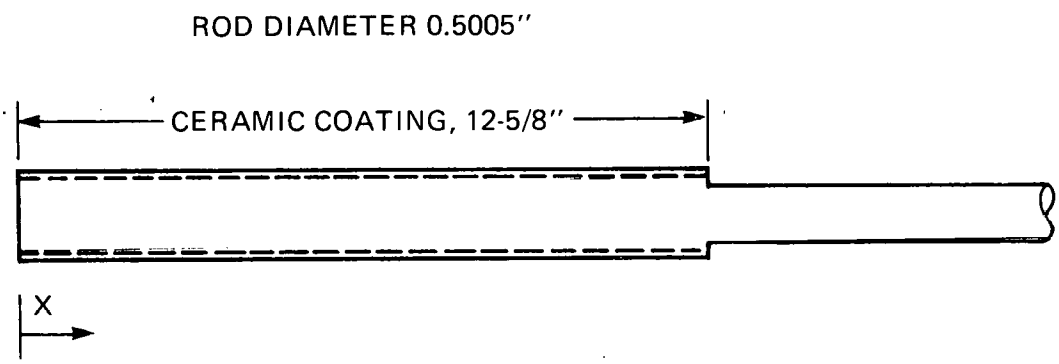

	OUTER DIAMETER	
X	VERNIER	MICROMETER
½	.506"	.5095"
1½	.506"	.5090"
2½	.510"	.5098"
3½	.506"	.5075"
4	.510"	.5100"
5	.507"	.5096"
6	.506"	.5085"
7	.507"	.5102"
8	.507"	.5089"
9	.506"	.5092"
10½	.508"	.5110"
11½	.506"	.5078"

Figure 4.5
THE COATED CENTER ELECTRODE

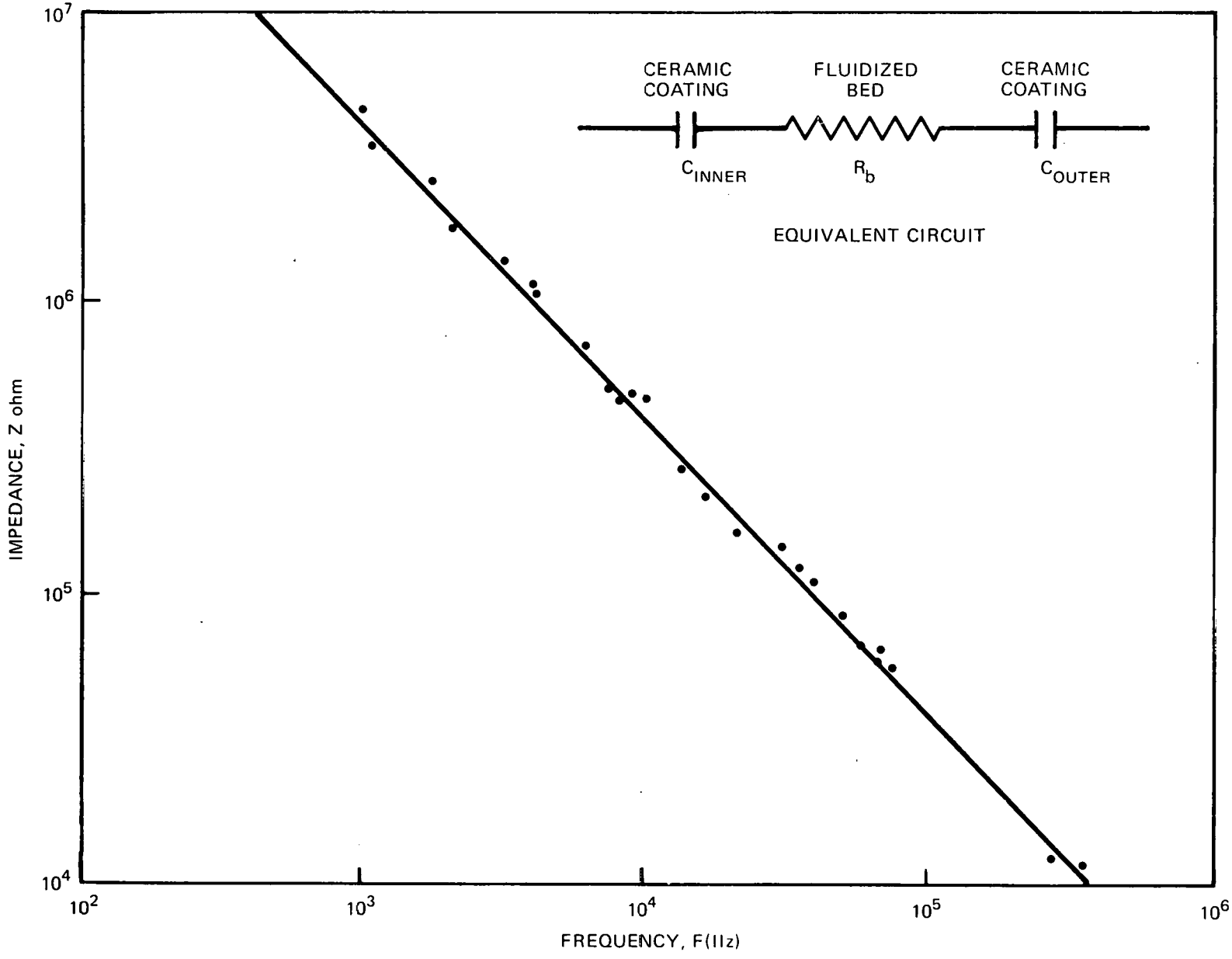

Figure 4.6
MEASURED VOLTAGE/CURRENT RELATIONSHIP

4.3 CONCLUSIONS

A theoretical model of capacitive heating of a fluidized bed was developed. This model takes into account the temperature dependency of thermal conductivity and diffusion coefficient. The model was incorporated into a computer program to determine the regimes of stability, to predict conversion efficiency, and to optimize key design parameters.

Testing with a steel-wall reactor indicates that fluidized particles can be heated by high-frequency capacitive-heating. A sudden bed impedance drop is observed during heating when the temperature reaches about 32°C. This behavior is unexplained at this time.

A glass-wall reactor was built and testing has begun. In general, fluidization was attained without any anomalous tendency. Additional qualitative tests will follow.

Tests with a ceramic-coated center electrode show that the coating maintained its electrical integrity.

4.4 PROJECTED QUARTERLY ACTIVITIES

4.4.1 THEORETICAL MODEL

The model will be used to generate bed performance. A simple model will also be developed for the electrical interaction in a bed and will be compared to the experimental results. This work will be documented.

4.4.2 EXPERIMENTAL WORK

Additional tests will be conducted with the glass-wall reactor to characterize fluidization behavior at various bed temperatures.

More work with the coated electrode will also be made to provide a complete electrical characterization of the system. The addition of a true-power meter will also aid in obtaining more precise electrical measurements.

Temperature measurements in the steel-wall reactor will resume. Because of the difficulty encountered with thermocouples, a trial use of thermisters is planned; if successful, thermisters will be installed throughout. All tests will be completed and findings documented.

4.5 REFERENCES

4.1 F. C. Everstein, et.al., J. Electrochem. Soc., 117, 7, p. 925, July, 1970.

4.2 A. K. Praturi, et.al., JPL Publication 77-38, July, 1977.

4.3 R. A. Suehla, NASA SP-3011, 1964.

4.4 R. C. Reid, J. M. Prausnitz, and T. K. Sherwood, The Properties of Gases and Liquids, McGraw-Hill, 1977.

4.5 F. C. Everstein, and B. H. Put, J. Electrochem. Soc., 120, 1, p. 106, January, 1973.

4.6 K. Kim, et.al., JPL Publication 77-25, June, 1977.

☆U.S. GOVERNMENT PRINGING OFFICE: 1978-740-094/1408